Isw2 and Ino80 chromatin remodeling factors regulate chromatin, replication, and copy number at the yeast ribosomal DNA locus

Sam Cutler[1,2], Laura J Lee[1,2], Toshio Tsukiyama[1*]

[1]Basic Sciences Division, Fred Hutchinson Cancer Research Center, Seattle, WA, United States of America

[2]Molecular and Cellular Biology Program, University of Washington, Seattle, WA, United States of America

* ttsukiya@fredhutch.org

Short title: Chromatin remodeling factors and the ribosomal DNA locus

Abstract

In the budding yeast *Saccharomyces cerevisiae*, ribosomal RNA genes are encoded in a highly repetitive tandem array referred to as the ribosomal DNA (rDNA) locus. The yeast rDNA is the site of a diverse set of DNA-dependent processes, including transcription of ribosomal RNAs by RNA Polymerases I and III, transcription of non-coding RNAs by RNA Polymerase II, DNA replication initiation, replication fork blocking, and recombination-mediated regulation of rDNA repeat copy number. All of this takes place in the context of chromatin, but relatively little is known about the roles played by ATP-dependent chromatin remodeling factors at the yeast rDNA. In this work, we report that the Isw2 and Ino80 chromatin remodeling factors are targeted to this highly repetitive locus. We characterize for the first time their function in modifying local chromatin structure, finding that loss of these factors affects the occupancy of nucleosomes in the 35S ribosomal RNA gene and the positioning of nucleosomes flanking the ribosomal origin of replication. In addition, we report that Isw2 and Ino80 promote efficient firing of the ribosomal origin of replication and facilitate the regulated increase of rDNA repeat copy number. This work significantly expands our understanding of the importance of ATP-dependent chromatin remodeling for rDNA biology.

Author Summary

To satisfy high cellular demand for ribosomes, genomes contain many copies of the genes encoding the RNA components of ribosomes. In the budding yeast *Saccharomyces cerevisiae*, these ribosomal RNA genes are located in the “ribosomal DNA locus”, a highly repetitive array that contains approximately 150 copies of the same unit, in contrast to the single copies that

suffice for most genes. This repetitive quality creates unique regulatory needs. Chromatin structure, the packaging and organization of DNA, is a critical determinant of DNA-dependent processes throughout the genome. ATP-dependent chromatin remodeling factors are important regulators of chromatin structure, and yet relatively little is known about how members of this class of protein affect DNA organization or behavior at the rDNA. In this work, we show that the Isw2 and Ino80 chromatin remodeling factors regulate two features of chromatin structure at the rDNA, the occupancy and the positioning of nucleosomes. In addition, we find that these factors regulate two critical processes that function uniquely at this locus: DNA replication originating from within the rDNA array, and the regulated increase of rDNA repeat copy number.

Introduction

In exponentially growing cells, the enormous cellular demand for ribosomes is reflected in the proportion of resources dedicated to their production. For example, the production of ribosomal RNAs (rRNAs) accounts for an estimated 60% of all transcriptional activity in cycling yeast cells [1]. Because single genomic copies of rRNA genes would not support such large volumes of transcriptional output, eukaryotic genomes have evolved to include highly repetitive clusters of rRNA genes, termed the ribosomal DNA (rDNA) locus. In a typical cell of the budding yeast *Saccharomyces cerevisiae*, the rDNA locus comprises approximately 150-200 tandem repeats (Fig 1A). Each repeat contains a 35S ribosomal RNA (rRNA) gene, transcribed by RNA Polymerase I (Pol I), and an inter-genic spacer (IGS), split into IGS1 and IGS2 regions by the 5S rRNA gene, which is transcribed by RNA Polymerase III (Pol III). Due to its large size and repetitive nature, the rDNA locus has unique regulatory needs, and the IGS1 and IGS2 regions contain genetic elements that are critical to addressing these needs.

Without an origin of replication (autonomously replicating sequence, or ARS), replicating the rDNA array would require replication forks to traverse multiple megabases of DNA from either end of the array. To avoid this, IGS1 contains a ribosomal ARS (rARS). As a consequence, the approximately 150 ARSs in a typical rDNA array account for nearly one third of all genomic origins of replication. Of these rARSs, only around 20% will fire in any given round of cell division [2, 3]. Because replication factors are limiting during each S-phase [4], firing of too many rARSs would take vital replicative resources away from other parts of the genome, raising the risk of delayed or incomplete replication. If too few rARSs fire, replication of the rDNA array may be delayed or incomplete [5]. Thus, properly striking this balance by regulating origin efficiency at the rDNA has critical consequences for global genome stability.

Genome stability is also affected by the size of the rDNA array [6]. Because of this, a mechanism exists to change the size of the array by adding or removing copies of the rDNA repeat if needed. The IGS2 region contains two genetic elements that are critical for this process: a bi-directional RNA Pol II promoter, E-pro, and a replication fork block (RFB). The RFB pauses replication forks moving through the IGS toward the 3' end of the 35S gene, but allows forks coming from within the adjacent 35S gene, and thus moving in the same direction as 35S transcription, to pass through or merge with paused forks. This activity is thought to prevent head-on collisions between replication machinery and densely loaded Pol I machinery in the highly transcribed 35S [3, 7]. In addition, forks paused at the RFB are the sites of targeted DNA double-strand breaks (DSBs). The level of transcription from the adjacent E-pro promoter influences the mechanism by which these targeted DSBs are repaired, which in turn influences whether a repeat is added to or removed from the rDNA array, or whether the copy number remains unchanged [8].

All DNA-dependent processes occurring at the rDNA, including transcription by multiple RNA polymerases, origin firing, and changes in rDNA copy number, happen in the context of chromatin structure. The Sir2 and Rpd3 histone deacetylases (HDACs) have well-established roles in regulating rDNA chromatin structure, origin activity, and copy number maintenance [5, 8-10]. In addition, rDNA biology is regulated by ATP-dependent chromatin remodeling factors, which use the energy of ATP hydrolysis to modify the position and histone composition of nucleosomes. In humans, the nucleolar remodeling complex (NoRC) positions nucleosomes and recruits histone methyltransferase and histone deacetylase activity to promote rDNA silencing [11, 12]. In yeast, the SWI/SNF [13], Isw1, Isw2, and Chd1 [14] complexes have been implicated in regulating transcription of rRNAs. Until now, no remodeling factors have been shown to modify chromatin structure at the yeast rDNA or to affect any DNA-dependent processes beyond rRNA transcription at this locus.

In this work, we show that the Isw2 and Ino80 ATP-dependent chromatin remodeling factors regulate chromatin structure at the rDNA. The Isw2 complex is known to slide nucleosomes over gene promoters [15], an activity that generally represses transcription, both for coding genes [16, 17] and antisense transcripts [18]. The Ino80 complex slides and evicts nucleosomes and removes the histone variant, H2A.Z [19-22]. Ino80 is also involved in regulating the checkpoint response following DNA damage, DNA damage repair, and DNA replication [23-25]. Isw2 and Ino80 function together to promote replication of late-replicating regions of the genome in the presence of replication stress and to attenuate the S-phase checkpoint response [26, 27]. Here, we show that both Isw2 and Ino80 are targeted to the ribosomal DNA locus in distinct patterns, primarily characterized by striking enrichment of Isw2 around the rARS and of Ino80 through the 35S gene. Further, we report for the first time that these remodeling factors affect local chromatin structure, as loss of the factors increases nucleosome occupancy in the 35S and alters the positioning of nucleosomes flanking the rARS. We find that loss of Isw2 and

Ino80 reduces the proportion of active rDNA repeats without affecting overall transcription of rRNAs, but that Isw2 and Ino80 positively contribute both to the efficiency of the rARS and to the rate of rDNA repeat copy number change. In sum, this study significantly expands our understanding of how ATP-dependent chromatin remodeling factors affect both chromatin structure and essential biological processes at the ribosomal DNA locus.

Results

The Isw2 and Ino80 chromatin remodeling complexes are targeted to the ribosomal DNA locus

All of the DNA-dependent processes that take place at the rDNA locus occur in the context of chromatin. Although HDACs such as Rpd3 and Sir2 have well-characterized functions in regulating chromatin structure, transcription, and copy number maintenance at the *S. cerevisiae* rDNA [8-10, 28], comparatively little is known about the roles played by ATP-dependent chromatin remodeling factors at this vitally important genomic locus. To address this, we performed chromatin immuno-precipitation followed by deep sequencing (ChIP-seq) to map where the Isw2 and Ino80 chromatin remodeling factors are targeted at the rDNA. We found that the namesake, catalytic subunit of Isw2 and Nhp10, a subunit wholly unique to the Ino80 complex [23], were both targeted to the rDNA (Fig 1B). The ChIP-seq signal for Isw2 was slightly above the genome-average throughout the 35S gene body. The pattern of targeting in the IGS included small peaks flanking the 5S gene and the region containing E-pro and RFB, but the most prominent signal was a striking, bimodal peak on top of and to one side of the rARS. Nhp10 was also present throughout the 35S gene body and showed a small peak around

the 5S. Each protein's ChIP-seq pattern at the rDNA was consistent with peaks elsewhere in the genome with regard to both shape and magnitude: Isw2 tended to have fairly defined peaks that rise well above the genome average, located in intergenic regions, and Nhp10 peaks were generally less prominent relative to the genome average and more diffusely spread throughout a transcription unit (Fig 1C). Given these distinct targeting patterns, we hypothesized that these ATP-dependent chromatin remodeling factors might have previously unknown functions at this highly repetitive, unique genomic locus.

Isw2 and Ino80 affect nucleosome occupancy over the 35S rRNA gene

In light of the established functions of the Isw2 and Ino80 complexes, we first asked whether these chromatin remodeling factors affect nucleosome occupancy within the rDNA locus, as this feature of chromatin structure has well-established importance at the rDNA. Individual rDNA repeats canonically exist in one of two discrete states, being either highly occupied with nucleosomes and transcriptionally inactive, or heavily depleted of nucleosomes and highly transcriptionally active [29-31]. We assessed how nucleosome occupancy at the rDNA is affected by these two chromatin remodeling factors with ChIP-seq of histone H3 in wild-type, *isw2*Δ, *nhp10*Δ, and *isw2*Δ *nhp10*Δ strains. This analysis revealed that nucleosome occupancy throughout the 35S gene body is appreciably increased in the *isw2*Δ *nhp10*Δ double mutant compared to wild-type and single deletion strains (Fig 2A, left panel). Notably, this is the part of the rDNA in which the ChIP-seq signals of both chromatin remodeling factors most significantly overlap, suggesting the possibility that these factors may work together in this region.

Given that rDNA repeats canonically exist in one of two discrete states that are associated with nucleosome occupancy, we hypothesized that the increased nucleosome occupancy in *isw2*Δ

*nhp10*Δ cells reflects a reduced ratio of active to inactive rDNA repeats. To test this, we used psoralen cross-linking, a well-established method in which DNA is treated with the DNA-intercalating compound, psoralen [29, 32]. Occupancy of chromatin by nucleosomes blocks incorporation of psoralen. Therefore, actively transcribed, nucleosome-depleted rDNA repeats become more heavily cross-linked with psoralen than inactive, nucleosome-occupied repeats. After digestion with appropriate restriction enzymes, Southern blotting, and hybridization with a probe targeting a region of the 35S gene unit, two discrete bands representing active and inactive repeats can be resolved [29, 32]. By this method, we found that *isw2*Δ *nhp10*Δ cells have a reduced proportion of active repeats compared to wild-type, *isw2*Δ, or *nhp10*Δ cells (Fig 2B), consistent with the observed increase in H3 occupancy in double mutant cells. Based on these results, we concluded that the Isw2 and Ino80 chromatin remodeling factors increase the ratio of active to inactive rDNA repeats.

Transcription of 35S ribosomal RNA is not affected by loss of Isw2 or Nhp10

Based on the reduced proportion of nucleosome-depleted rDNA repeats in the *isw2*Δ *nhp10*Δ mutant, we hypothesized that these cells would also show reduced levels of 35S rRNA transcription. The 35S is transcribed as a single long transcript before being cleaved and folded in a series of processing steps to yield mature 18S, 5.8S, and 25S RNAs [33]. Because mature rRNAs are components of ribosomes and thus highly stable and abundant, nascent RNA needs to be measured to assess the transcription rate of rRNAs. The External Transcribed Spacer 1 (ETS1) and Internal Transcribed Spacer 1 (ITS1) sections of the 35S gene are transcribed but removed at early stages of rRNA processing. Levels of these RNA sequences thus reflect levels of nascent rRNA and are commonly used to measure the rate of 35S transcription [34, 35]. Adopting this approach, we performed reverse-transcription quantitative PCR (RT-qPCR)

targeting parts of the ETS1 and ITS1 regions of the 35S pre-rRNA (Fig 2A). As expected, we found significantly reduced levels of both ETS1 and ITS1 in an *rpa49* deletion mutant, a strain known to have a reduced rate of RNA Pol I transcription [35, 36]. To our surprise, we did not see evidence of a significant difference in rates of 35S transcription in *isw2*Δ *nhp10*Δ compared to wild-type (Fig 2C). To confirm this unexpected result by an independent method, we next performed ChIP-seq analysis of the Pol I subunit RPA190, and observed virtually identical profiles in *isw2*Δ *nhp10*Δ and wild-type strains, with regard to both shape and overall levels (Fig 2D). Based on these results, we concluded that *isw2*Δ *nhp10*Δ cells exhibit no significant defects in the rate of 35S transcription despite the observed differences in nucleosome occupancy and the proportion of nucleosome-occupied rDNA repeats in these mutants.

Isw2 and Ino80 affect nucleosome positioning in the rDNA inter-genic spacer

In addition to nucleosome occupancy, nucleosome positioning is known to be affected by both of these chromatin remodeling factors [15, 20]. Therefore, we assessed nucleosome positioning at the rDNA by micrococcal nuclease (MNase) digestion followed by deep sequencing (MNase-seq). We interpret each size-selected, paired-end read as coming from a nucleosome-protected fragment of DNA, and so from each paired-end read, the nucleosomal dyad center was inferred and plotted, resulting in the profiles shown (Fig 3A). By this method, nucleosome positions appear strongly shifted at known Isw2 targets in *isw2*Δ and *isw2*Δ *nhp10*Δ mutants (S1 Fig). In contrast, no gross differences in nucleosome positions are observed throughout the 35S gene body (S2A Fig) or in the rDNA inter-genic spacer region (Fig 3A). Within the highly repetitive rDNA, sequencing data must be interpreted carefully, however, as it represents an average of the signal at all ~150 rDNA repeats in all cells sampled, and nucleosomes in only a fraction of those repeats may change positions in any given cell.

To refine our analysis, we compared MNase-seq profiles for the tested strains using ribbon plots in which the primary line shows the average signal at each base pair across multiple biological replicates, and the ribbon represents the standard error of the mean for those replicates (Fig 3B). This method revealed striking differences in nucleosome positioning at the rDNA for two pairs of nucleosomes. One pair is in between the 35S promoter and the rARS, with each nucleosome substantially overlapping one of the two sub-peaks of the highly prominent Isw2 peak (Fig 3B, left panel, identified as nucleosomes 1 and 2). The other pair of affected nucleosomes is in the region between the rARS and the 5S gene, overlapping half of the short Isw2 peak encompassing the 5S (Fig 3B, right panel, nucleosomes 3 and 4). Each of these four MNase-seq dyad peaks appears to have two sub-species of nucleosome positions. We interpret each of these distinct sub-species as representing one of two distinct positions occupied by that nucleosome in different individual rDNA repeats in the array. Each of the four genotypes tested has a characteristic pattern of the relative heights of these two sub-species, which we propose reflects different proportions of rDNA arrays containing nucleosomes at either position.

At nucleosome 1, *isw2*Δ and *isw2*Δ *nhp10*Δ cells virtually only have sub-species 1*b*, while both wild-type and *nhp10*Δ cells also have a significant signal for sub-species 1*a*. At nucleosome 2, wild-type cells predominantly have sub-species 2*a*, whereas *isw2*Δ cells have more prominent signals for 2*b*, and *nhp10*Δ and *isw2*Δ *nhp10*Δ cells have roughly similar ratios of each sub-species. Nucleosome 3 resembles nucleosome 1, in that for some strains – in this case, wild-type, *isw2*Δ, and *nhp10*Δ cells – there is essentially only one sub-species, 3*b*, whereas only *isw2*Δ *nhp10*Δ cells have a small but distinct sub-species 3*a*. For nucleosome 4, wild-type and *isw2*Δ cells are very similar, with 4*b* dominating and 4*a* and 4*c* of similar, lower prominence, while *nhp10*Δ cells have similar levels of 4c but proportionally reduced 4*a* and 4*b* peaks. Again, the double mutant is the most different among the tested strains, as 4*c* is barely detectable,

while 4*a* is on par with 4*b* in *isw2*Δ *nhp10*Δ cells. In sum, the overall trend among these mutants is that in *isw2*Δ *nhp10*Δ cells, any given rDNA repeat is more likely to have nucleosomes positioned such that they are encroaching on the rARS. In contrast, in both *nhp10*Δ and wild-type cells, these same nucleosomes are more likely to be positioned farther away from the rARS, and in *isw2*Δ cells these nucleosomes have profiles somewhere in between wild-type and the double mutant.

Nucleosomes 3 and 4 are located in between the rARS and the 5S rRNA gene. Thus, the positioning shifts of these nucleosomes relative to the rARS also happen, in the opposite direction, relative to the 5S. In addition, there were slight strain specific differences at the nucleosome partially overlapping the 5S: sub-species *a* is higher than *b* in wild-type, *isw2*Δ, and *nhp10*Δ cells, but the sub-species are roughly equivalent in *isw2*Δ *nhp10*Δ cells (S2B Fig). These differences in nucleosome positioning suggested that Isw2 and Ino80 might alter nucleosomes to regulate 5S transcription. Because this gene is only 120 bp in length and undergoes only minor processing before incorporation into ribosomes, it is difficult to distinguish between mature and nascent 5S rRNA transcripts. Therefore, to assess 5S transcription, we performed RNA Pol III ChIP-seq. Similarly to RNA Pol I levels at the 35S, Pol III levels at the 5S did not differ between wild-type and *isw2*Δ *nhp10*Δ cells (S2C Fig). Thus, we conclude that Isw2 and Ino80 do not significantly affect transcription of ribosomal RNAs despite changes in chromatin structure around the transcription units.

It has been shown that the strength of MNase digestion can affect nucleosome mapping results, especially for nucleosomes that are highly MNase sensitive [37]. Because the differences in MNase-seq signal at the rDNA locus were more subtle than what is typically observed at single-copy loci, we sought to ensure that these differences are not due to differential MNase sensitivity of these nucleosomes. To this end, we compared the MNase-seq profiles for these

nucleosomes in wild-type and *isw2*Δ *nhp10*Δ strains using three different concentrations of MNase (Fig 3C, S3 Fig). The overall shapes of the MNase-seq profiles varied depending on MNase concentrations used. However, at any specific degree of digestion, the relative heights of nucleosomal sub-species for wild-type versus *isw2*Δ *nhp10*Δ cells matched the patterns described above. These results confirmed that the observed shifts in nucleosome positions in mutants were not due to differential MNase sensitivity of these nucleosomes.

Isw2 and Ino80 facilitate efficient firing of rDNA origin of replication

The prominent Isw2 peak around the rARS coupled with the shrinkage of NDRs over the rARS in chromatin remodeling factor mutants led us to ask whether origin activity is affected by these factors. To address this question, we performed two-dimensional (2D) gel electrophoresis probing activity of the rARS (Fig 4A, [3]). The Y arc of the 2D gel is comprised of restriction fragments in the process of being passively replicated, and the bubble arc of restriction fragments in which an origin of replication has actively fired. Therefore, the ratio of bubble to Y arc signals from asynchronously growing cells reflects the ratio of actively to passively replicated restriction fragments, and thus of origin efficiency. By this method, the ratio of rARS bubble to Y arc signal, and thus rARS origin efficiency, was greatest in the wild-type and slightly reduced in *isw2*Δ cells. In contrast, origin efficiency was moderately reduced in *nhp10*Δ cells and even more reduced in *isw2*Δ *nhp10*Δ double mutants (Fig 4B). These results indicate that the Isw2 and Ino80 chromatin remodeling factors promote the efficient firing of the ribosomal origin of replication.

Isw2 and Ino80 affect replication fork pausing at the rDNA Replication Fork Block

One unique aspect of DNA replication at the rDNA locus is the presence of the replication fork block (RFB). When bound by the Fob1 protein, the RFB directionally blocks the passage of replication forks from the IGS into the 3' end of the 35S gene body, preventing head-on collisions between the replication machinery and the densely-loaded transcriptional machinery moving through the highly transcribed 35S genes [3, 7]. However, replication forks moving in the same direction as that transcriptional machinery can pass through the RFB, thus allowing for complete replication of the rDNA array. Replication fork blocking at the RFB can be detected by 2D gels as a distinct spot on the left end of the Y arc (Fig 4A). A light exposure of the 2D gel revealed reduced replication fork pausing at the RFB in remodeling factor mutants (Fig 4C). Quantifying the degree of replication fork blocking relative to the amount of loaded DNA is difficult, however, because of the large difference in the signal intensities of the RFB and the 1N spot, which represents non-replicating restriction fragments and serves as a reference for normalization. To accurately measure the degree of replication fork blocking at the RFB, we analyzed occupancy of Pol2, a subunit of DNA Polymerase epsilon, by ChIP-seq in asynchronously growing cells, an established method for globally measuring replication fork pausing [38]. Pol2 levels, and thus pausing, at the RFB are comparable to wild-type in *isw2*Δ cells, but are reduced in *nhp10*Δ and *isw2*Δ *nhp10*Δ mutants (Fig 5A), similar to what we observe for rARS efficiency. In contrast, Pol2 signals at known pause sites such as *PDC1* are very similar across all tested strains (S4 Fig), suggesting that differences in pausing at the rDNA RFB are unique to that locus, and not a genome-wide phenomenon.

Because Fob1 binding at the RFB is required for pausing at this locus, we next asked whether Isw2 and Ino80 affect replication fork blocking at the RFB by altering the level of Fob1 binding. To this end, we performed ChIP of Fob1 followed by qPCR using primers flanking the RFB. This

experiment revealed that the *nhp10*Δ strain, which exhibits the lowest level of replication fork pausing, also shows the lowest levels of Fob1 occupancy (Fig 5B). However, *isw2*Δ *nhp10*Δ cells, which have similarly low levels of pausing, have considerably higher levels of Fob1, on par with *isw2*Δ cells and above that of the wild-type cells. Therefore, the level of Fob1 binding alone cannot explain the strain-specific differences we observe in replication fork pausing at the RFB.

Isw2 and Ino80 affect the rate of rDNA copy number change

Replication fork pausing at the RFB is an essential step in the mechanism by which rDNA copy number is regulated. With some frequency, a targeted DNA double-strand break (DSB) will occur at replication forks paused at the RFB. Depending on how this DSB is repaired, an rDNA repeat can be removed from or added to the rDNA array, or there can be no change in rDNA copy number. Thus, Fob1-dependent replication fork pausing is a critical feature of rDNA copy number change. Given the differential pausing at the RFB in our remodeling factor mutants, we wondered whether Isw2 and Ino80 affect rDNA copy number change. To answer this question, we employed a strain in which endogenous *FOB1* has been deleted and the rDNA array reduced to 20 repeats. In the absence of Fob1, there is no pausing at the RFB, stabilizing the rDNA copy number. These cells can survive with 20 copies of the rDNA, but introduction of Fob1 via a plasmid causes rapid increase in the number of rDNA repeats via homologous recombination until the rDNA array reaches a normal size of approximately 150 copies [8]. Starting with a *fob1* strain with 20 copies of the rDNA, *ISW2*, *NHP10*, or both genes were deleted. The Fob1 gene was then reintroduced on a plasmid, and the cells were cultured continuously under selection for almost 200 generations, with samples taken at multiple time points. The copy number of rDNA repeats was monitored by CHEF gel electrophoresis followed by Southern blot analysis using a probe against the rDNA locus.

Although all four strains began to increase their rDNA copy number immediately following introduction of plasmid-borne Fob1, each of the strains behaved differently (Figs 6A, B). In wild-type and *isw2*Δ cells, and to a slightly lesser degree in *nhp10*Δ cells, there was a significant jump in copy number at around 35 generations after Fob1 re-introduction, the earliest time point we were able to sample. In contrast, the double mutant exhibited only a very small increase in copy number at 35 generations. After nearly 200 generations in the presence of Fob1, both the wild-type and *isw2*Δ strains had recovered essentially wild-type rDNA copy number of around 150 copies, and *nhp10*Δ was close to this number. In contrast, *isw2*Δ *nhp10*Δ had barely reached 100 copies by this time point. Based on this data, we conclude that Isw2 and Ino80 facilitate the regulated increase of rDNA copy number in the rDNA array, and that their loss reduces the rate at which rDNA copy number can be increased in a population of cells.

Discussion

The ribosomal DNA locus is the evolutionarily conserved site of many different DNA-dependent processes, all of which must be carefully balanced. Sufficient rRNA must be transcribed to support ribosome biogenesis, but without interfering with faithful replication of the rDNA [1]. The rDNA array must be fully replicated, while still allowing for the replication of other parts of the genome [5]. The size of the rDNA array must be carefully maintained through recombination, yet the array must be protected from unintended recombination despite its highly repetitive nature. Despite many studies detailing these complex processes, relatively little is known about how ATP-dependent chromatin remodeling factors dynamically regulate chromatin structure at the *S. cerevisiae* rDNA locus to allow for these processes to occur. It has been shown that the

SWI/SNF complex localizes to the rDNA and that deletion of its Snf6 subunit reduces 35S rRNA transcription [13]. In addition, it was shown that Isw2, Isw1, and Chd1 are present at the rDNA, and that their simultaneous deletion reduces 35S rRNA transcriptional termination [14]. However, the nature of chromatin regulation by these remodeling factors at the rDNA locus remains unknown, as does their involvement in processes beyond transcription of rRNA. In this study, we show that in addition to Isw2, the Ino80 ATP-dependent chromatin remodeling factor is targeted to this highly repetitive genomic locus. We show for the first time that these factors modify local chromatin structure at the levels of nucleosome occupancy, the ratio of nucleosome-occupied to nucleosome-depleted rDNA repeats, and nucleosome positioning. In addition, we find that these chromatin remodeling factors affect two critical activities that take place at the rDNA: replication initiation from the ribosomal ARS, and rDNA array amplification.

Our data indicate that Isw2 and Ino80 do not affect overall levels of 35S rRNA transcription, a result that initially surprised us. According to the prevailing model, nucleosome occupancy through the 35S gene body dictates 35S transcription, as rDNA repeats that are heavily occupied with nucleosomes are transcriptionally silent, while repeats that are depleted of nucleosomes are transcriptionally active. Thus, based on the increased nucleosome occupancy and reduced proportion of psoralen-accessible rDNA repeats observed in *isw2*Δ *nhp10*Δ cells relative to other tested strains, we expected that 35S rRNA transcription would be correspondingly decreased in the double mutant. The lack of an effect on transcription may be explained by the robustness of 35S transcriptional regulation: when one element of this system is disrupted, another element is adjusted to maintain the desired level of transcription. For example, in a *S. cerevisiae* strain in which the rDNA array has been reduced from a normal size of ~150 copies down to ~40 copies, loading of RNA Pol I on any given active repeat is increased, such that there is no net decrease in 35S transcriptional output [30]. Similarly, in mammalian cells, inducing silencing of some rDNA repeats by depletion of UBF leads to a

compensatory increase in transcription per active repeat [39]. We therefore speculate that the robust homeostatic regulation of rRNA transcription overcomes changes in nucleosome occupancy in *isw2*Δ *nhp10*Δ cells, reacting to a reduced proportion of active repeats by increasing RNA Pol I transcription in each active unit. This would produce no net alteration in rRNA production compared to wild-type cells. We also note that our H3 ChIP-seq data reveals that the nucleosome-depleted region (NDR) in the 35S promoter is much deeper in *isw2*Δ *nhp10*Δ cells than in wild-type or single mutant cells (S5 Fig). According to a general paradigm of RNA Pol II transcription, promoter NDR depth correlates positively with transcription [40, 41]. This deepened NDR in *isw2*Δ *nhp10*Δ cells may reflect significantly increased loading of Pol I transcriptional machinery in each active repeat, as needed to maintain proper levels of 35S transcription despite the reduced number of active repeats.

A critical transcriptional regulator at the mammalian rDNA is the Nucleolar Remodeling Complex (NoRC), which contains SNF2h, the mammalian orthologue of yeast Isw2. Among other activities that influence rRNA transcription, this complex shifts the nucleosome at the promoter of the 45S rRNA gene, the mammalian orthologue of the yeast 35S, into a transcriptionally repressive position [12]. Notably, we see nearly identical nucleosome positioning profiles at the comparable nucleosome in *isw2*Δ and *isw2*Δ *nhp10*Δ cells compared to wild-type cells (S2D Fig). This finding, in conjunction with our observing no differences in rRNA transcription in these deletion strains, distinguishes the Isw2-mediated regulation of the yeast rDNA from the NoRC-mediated regulation of the mammalian rDNA.

While we find that loss of Isw2 and Ino80 does not affect net rRNA transcription, we do find that their loss reduces the activity of the rARS. There are multiple reports that chromatin structure around replication origins significantly affects DNA replication. Blocking an ARS with a nucleosome reduces the efficiency of that ARS [42], and proper positioning of nucleosomes

435 adjacent to an ARS is important for replication initiation [43]. Compared to naked DNA,
436 chromatinized DNA facilitates much greater origin selectivity at the stage of origin licensing,
437 suggesting that chromatin structure regulates which origins fire during S-phase [44]. Consistent
438 with these findings, ATP-dependent chromatin remodeling factors contribute to regulating
439 replication initiation. For example, the SWI/SNF complex is targeted to a subset of origins in
440 HeLa cells [45] and facilitates replication initiation at one out of four natural ARSs tested in a
441 mini-chromosome maintenance assay in *S. cerevisiae* [46]. By applying an *in vitro* replication
442 assay to nucleosomal templates remodeled by different chromatin remodeling factors, a recent
443 study found that most factors permitted origin licensing, but that Isw2 and Chd1 prevented it
444 [47]. As far as we know, however, there have been no reports of chromatin remodeling factors
445 affecting both chromatin structure and replication initiation at a specific origin of replication at its
446 natural genomic locus *in vivo*.
447
448 We report that loss of *ISW2* and *NHP10*, individually and together, reduced the efficiency of the
449 rARS during logarithmic growth conditions in rich medium. We found that *isw2*Δ *nhp10*Δ cells
450 have the most robust differences in nucleosome positioning compared to wild-type cells, with a
451 clear trend of an enrichment for nucleosomes in positions that encroach on the rARS. These
452 same cells have the most reduced efficiency at this ARS compared to wild-type. This effect is
453 reminiscent of the behavior of Isw2 at Pol II-transcribed genes targeted by Isw2. At such genes,
454 when *ISW2* is deleted, NDRs at the end of the gene targeted by Isw2 tend to widen, and nearby
455 non-coding transcription increases, suggesting that this remodeling factor typically functions to
456 narrow these NDRs and repress non-coding transcription [18]. We observe a similar but
457 oppositely oriented trend at the rARS, as our data suggest that the NDR containing the ARS
458 overall becomes narrower and origin efficiency goes down in *isw2*Δ *nhp10*Δ cells, suggesting a
459 normal function of these factors in keeping this NDR wide and thus permissive to replication
460 initiation. We also note that although we see intermediate effects on both nucleosome

positioning and efficiency of the rARS in *isw2*Δ and *nhp10*Δ single mutant cells, there does not appear to be a clear additive effect that accounts for what we observe in the double mutant. Although *isw2*Δ cells have more rARS-encroaching nucleosomes than *nhp10*Δ cells, efficiency of the rARS appears greater in *isw2*Δ cells than in *nhp10*Δ cells. Thus, it appears that nucleosome positioning around the rARS can only partially account for the effect these remodeling factors have on efficiency of the rARS. Reduced rARS efficiency in our mutants may also be partially explained by the altered ratio of transcriptionally active to inactive rDNA repeats. Evidence suggests that rARSs are more likely to fire when they are adjacent to actively transcribed rDNA repeats [48]. In our proposed model, the proportion of actively transcribed repeats is reduced in *isw2*Δ *nhp10*Δ cells, and thus a reduced proportion of rARSs in the array are adjacent to actively transcribed repeats. This may contribute to the reduced origin efficiency we observe in these mutants.

In addition to regulating rARS activity, a cell must carefully calibrate the size of the rDNA array. This highly repetitive locus must be large enough to allow for the transcription of sufficient ribosomal RNA to satisfy a cell's demand for ribosomes; in a typical yeast cell, approximately 75 copies of the rDNA are actively transcribed to satisfy this demand [1]. However, those 75 copies of the rDNA repeat must be insufficient under some circumstances, as a typical yeast rDNA array contains around 150 copies of the rDNA repeat. According to the prevailing model, these additional copies are necessary to maximize genome stability. Active ribosomal RNA genes are transcribed at extremely high levels, with densely loaded transcriptional machinery. This presents an obstacle to the repair of damage to the underlying DNA, and persistent, un-repaired damage to the rDNA array delays complete replication of the genome and progression through S-phase [6]. Thus, to maximize genome stability, the rDNA array must be large enough to support sufficient rRNA transcription without requiring all repeats to be actively transcribed. This requirement imposes a lower limit on the optimal size of the rDNA array. Similarly, the array

cannot exceed a certain size. If the rDNA grows too large, its complete replication would require an excessively large proportion of the finite pool of replisome components available during each S-phase, depriving other parts of the genome of those replication factors [5]. In addition, evidence suggests that having a smaller rDNA array improves growth during persistent replication stress, perhaps by making more of the limiting replication factors available to other parts of the genome [49]. Thus, the number of repeats in the rDNA locus must be actively managed by the cell to facilitate optimal transcriptional output and maximize genome stability. Most of our knowledge about the mechanism of rDNA copy number change comes from studying the cellular response to a significant perturbation in copy number. For example, if an rDNA array is artificially truncated, it will steadily increase until it reaches a normal size [50]. Conversely, the rDNA array will shrink when the *RPA135* subunit of RNA Pol I is deleted [50, 51], when the activity of the origin recognition complex is compromised [52], or when a number of other replication factors are lost [49]. Together, these studies demonstrate that maintenance of the size of the rDNA is a vital process that is actively regulated by the cell.

In this study, we describe a nearly two-fold reduction in the rate of copy number increase in *isw2*Δ *nhp10*Δ cells relative to wild-type cells, and moderate reductions in the rate of increase in *isw2*Δ and *nhp10*Δ cells. This is the first demonstration of any ATP-dependent chromatin remodeling factors contributing to the regulation of rDNA copy number change. We show that these remodeling factors affect Fob1 binding and replication fork pausing at the RFB, two critical steps in the process of copy number change, but the effects on these activities do not clearly correlate with the effects on the rate of copy number change we observe in the same mutants. Therefore, we do not believe the remodeling factors influence copy number change exclusively through replication fork pausing or Fob1 binding. Another critical step in this process is the repair of the targeted DNA double strand break (DSB) that takes place at RFB-paused replication forks. In light of a well-documented role for Ino80 in DSB repair [21, 53, 54], it is

possible that the striking defect in copy number increase we observe may result in part from mis-regulation of the recombination-based repair of these DSBs. In the absence of *NHP10*, there may be some mild defect in homologous recombination (HR) that may be partially compensated for by otherwise normal chromatin structure created by Isw2. However, in the double mutant, HR repair defects may become too significant to facilitate the desired recombination rate at rDNA.

In addition to this possible direct involvement of the remodeling factors in copy number increase, the effect we observe may be indirect. Our data suggest that in the absence of Isw2 and Ino80, the ratio of active to inactive rDNA repeats is reduced. In light of work showing that rARSs are more likely to fire when they are adjacent to actively transcribed rDNA repeats [48], we proposed above that this reduced proportion of active repeats could explain the reduced efficiency of the rARS in *isw2*Δ *nhp10*Δ cells. It has also been shown that copy number change events require firing of the rARS adjacent to the RFB at which a replication fork is paused, a DSB is induced, and then repaired. This same study found that the efficiency of the ARS in the IGS correlates with the rate of copy number increase [55]. Accordingly, it is possible that the reduced ratio of active to inactive repeats in the double mutant causes a change in rARS efficiency, which in turn reduces the frequency of copy number change events, thus accounting for the reduced rate of copy number increase in the double mutant cells. In sum, this work establishes a novel role for ATP-dependent chromatin remodeling factors in strongly influencing rDNA biology, including the process of rDNA copy number change.

Materials and Methods

538 **Yeast strains and media**

539 Strains used are listed in S1 Table. Strains generated using standard gene replacement
540 protocols. Unless otherwise indicated, yeast cells were grown in YEPD medium (2% Bacto
541 Peptone, 1% yeast extract, 2% glucose). All strains *MAT***a** W303-1a.

542

543 **Chromatin immunoprecipitation and micrococcal nuclease digestion followed by deep**
544 **sequencing**

545 Chromatin immunoprecipitation (ChIP) and micrococcal nuclease (MNase) digestion were
546 performed as described previously [58]. For H3-ChIP experiments, anti-H3 C-term antibody
547 (Abcam catalog # ab1791) was used; for all other ChIPs, the targeted protein was epitope-
548 tagged with FLAG, and immuno-precipitated using anti-FLAG monoclonal antibody (Sigma
549 catalog # F3165). All Isw2 ChIP-seq performed on a FLAG-tagged, catalytically inactive allele of
550 *ISW2* as previously described [59]. All libraries were constructed using the Nugen Ovation
551 Ultralow System V2 (catalog # 0344-32) and then subjected to single-end (ChIP-seq) or paired-
552 end (MNase-seq) sequencing, with 50 bp read length, on Illumina Hi-Seq 2500. Ribbon plots,
553 bar graphs, and line graphs were generated with the ggplot2 R package (http://ggplot2.org/). For
554 all depictions of deep-sequencing data at the rDNA, a single copy of the rDNA locus is shown.
555 Our reference genome contains two copies of the rDNA, and any read mapping to the rDNA is
556 randomly assigned to one of these 2 copies. Thus, sequencing data reflects the average signal
557 across all rDNA repeats in all cells sampled.

558

559 **Reverse Transcription- and ChIP-quantitative PCR**

560 RNA was isolated using hot acid phenol, then cleaned up with the Qiagen RNEasy Cleanup Kit
561 (catalog # 74204) plus on-column treatment with DNase I (Qiagen catalog # 79254). cDNA was
562 generated from the RNA using Superscript III Reverse Transcriptase (ThermoFisher catalog #
563 18080093). Quantitative PCR was performed on both cDNA and ChIP DNA using 2x Power

564 SYBR Master Mix (Fisher Scientific catalog # 4367659) run on the ABI QuantStudio5 Real Time
565 PCR System machine.
566
567 **Psoralen Crosslinking**
568 Assay was performed as previously described [10, 28, 32]. Cells were grown to mid-log phase
569 (OD_{660} = 0.5-0.7), approximately $3x10^8$ cells were collected, washed twice with ice cold water,
570 and then re-suspended in 1.4 ml cold TE buffer. Cells were transferred to 6 well plates, and 70
571 ul of psoralen (200 ug/ml in 100% ethanol) was added to the cells. On ice, the plates were
572 irradiated with 365 nm UV for five minutes. Psoralen addition followed by UV irradiation was
573 repeated four additional times, for a total of five rounds. Cells were collected, washed in water,
574 spheroplasted with zymoylase 100T, and washed in spheroplast buffer. The pellet was lysed by
575 re-suspension in TE buffer with 0.5% SDS and then treated with Proteinase K overnight at
576 50°C. DNA was extracted with Phenol:Chloroform:IAA, ethanol precipitated, and then digested
577 for at least 3 hours with EcoRI-HF. Samples were treated with RNase A at 37°C for 30 minutes,
578 ethanol precipitated, quantified, and then run in 1.3% LE agarose gels in 0.5X TBE for 24 hours
579 at 60V. Gels were irradiated for two minutes per side with a Stratagene Stratalinker, transferred
580 to a GeneScreen Plus membrane in 10x SSC, and then hybridized with a probe contained
581 within a EcoRI restriction fragment in the rDNA ETS1. Membranes were visualized using a
582 Typhoon Phosphor Imager, and images were visualized using ImageJ software.
583
584 **2D gel electrophoresis**
585 DNA sample preparation based on the Brewer/Raghuraman lab protocol (http://fangman-
586 brewer.genetics.washington.edu/plug.html). Cells were grown to mid-log phase (OD_{660} = 0.5-
587 0.7), sodium azide added to 0.1% final concentration, and then cultures were washed in water.
588 Cell pellets were re-suspended in 50 mM EDTA, mixed with an equal volume of 1.0% Low-Melt
589 Agarose (BioRad catalog # 161-3111), and pipetted into plug molds. Cells in plugs were

spheroplasted with 0.5 mg/ml Zymolyase 20-T, thoroughly washed, and stored in TE at 4°C. Plugs were digested with NheI for 5 hours at 37°C, then run in 0.4% agarose gels in TBE at 1 V/cm for 22 hours at room temperature. Gels were stained with ethidium bromide (EtBr), visualized with UV, and the desired size range for each sample was identified in the gel and physically cut out. This piece of gel was then rotated 90° and placed in a new gel tray, and warm 1.1% agarose in TBE was poured around it. This gel was then run at 5 V/cm for 6 hours at 4°C. After running, the gel was visualized, transferred onto a GeneScreen Plus membrane (Perkin Elmer, catalog # NEF986001PK), and hybridized with a probe encompassing the RFB.

rDNA copy number change assay

Strains were made from YSI102 [6], in which the endogenous *FOB1* gene had been deleted, and the number of rDNA repeats reduced to 20 copies. From the 20-rDNA-copy *fob1* parent, *isw2*Δ, *nhp10*Δ, and *isw2*Δ *nhp10*Δ strains were generated. Separately, the *FOB1* gene was cloned into the pRS426 plasmid using Gibson cloning. Either this *FOB1*-pRS426 plasmid or a pRS426 plasmid with no *FOB1* gene was then transformed into each 20-copy strain and plated on yeast complete (YC) –URA medium with 2% glucose. Individual transformants were re-streaked on selective medium, presence of the desired plasmid was confirmed by PCR, and then transformants were inoculated into liquid YC –URA + 2% glucose. Cultures were allowed to reach saturation, and then aliquots were collected, washed in cold 50 mM EDTA, and cell pellets were frozen in liquid nitrogen and stored at -80°C. From the remaining saturated cultures, all strains were diluted by the same factor, then allowed to grow back to saturation, at which point the next time point would be collected, up to ~200 generations. Generations were calculated from the base 2 log of the dilution factor applied at each passage (e.g. a saturated culture diluted by a factor of 1,024 into the same volume of medium would require 10 generations to return to saturation).

615

616 **Clamped Homogenous Electric Field (CHEF) gel electrophoresis and Southern blotting**

617 Samples for CHEF gels were prepared in agarose based on a previously described method
618 [60]. Frozen cell pellets were thawed in room-temperature water, re-suspended in 100 mM
619 EDTA, then mixed with 0.8% Low-Melt Agarose and 25 mg/ml zymolyase 20T. This mixture was
620 pipetted into plug molds, allowed to solidify at 4°C, then washed with a series of buffers
621 (Solution V: 500 mM EDTA pH 7.5, 10 mM Tris pH 7.5; Solution VI: 5% sarcosyl, 5 mg/ml
622 proteinase K, 500 mM EDTA pH 7.5; Solution VII: 2 mM Tris pH 7.5, 1 mM EDTA, pH 8.0).
623 Before being run, plugs were incubated for approximately 30 minutes in TBE running buffer at
624 4°C before being placed on gel comb teeth, positioned in gel mold, and then warm 0.8% 0.5x
625 TBE was poured. CHEF gel was run on a CHEF-DR II with a program adapted from Ide *et al*
626 MCB 2007: Block 1 = 2.0 V/cm, pulse time of 1,200 seconds to 1,400 seconds, total run time
627 72 hours; Block 2 = 6.0 V/cm, pulse time of 25 seconds to 146 seconds, total run time 7.5
628 hours. After electrophoresis, gels were incubated with 0.5 ug/ml EtBr in running buffer for 30-45
629 minutes, UV-irradiated with a Stratagene Stratalinker to nick DNA, transferred onto HyBond N+
630 positively charged membrane (GE, catalog # RPN303B), and hybridized with a probe targeting
631 the RFB.

632

633

634 ## Acknowledgments

635

636 We are grateful to members of the Brewer/Raghuraman lab, especially Bonny Brewer, MK
637 Raghuraman, Joe Sanchez, and Liz Kwan, for help with experimental design and
638 troubleshooting, as well as conceptual discussion and feedback, and members of the Smith lab,
639 especially Randy Hyppa, for help with CHEF gels. We thank Takehiko Kobayashi for strains

used in this study. Finally, we thank members of the Tsukiyama lab for helpful discussion and commentary on this manuscript.

References

1. Warner JR. The economics of ribosome biosynthesis in yeast. Trends Biochem Sci. 1999;24(11):437-40. Epub 1999/11/05. PubMed PMID: 10542411.

2. Walmsley RM, Johnston LH, Williamson DH, Oliver SG. Replicon size of yeast ribosomal DNA. Mol Gen Genet. 1984;195(1-2):260-6. Epub 1984/01/01. PubMed PMID: 6387390.

3. Brewer BJ, Fangman WL. A replication fork barrier at the 3' end of yeast ribosomal RNA genes. Cell. 1988;55(4):637-43. Epub 1988/11/18. PubMed PMID: 3052854.

4. Mantiero D, Mackenzie A, Donaldson A, Zegerman P. Limiting replication initiation factors execute the temporal programme of origin firing in budding yeast. Embo j. 2011;30(23):4805-14. Epub 2011/11/15. doi: 10.1038/emboj.2011.404. PubMed PMID: 22081107; PubMed Central PMCID: PMCPMC3243606.

5. Yoshida K, Bacal J, Desmarais D, Padioleau I, Tsaponina O, Chabes A, et al. The histone deacetylases sir2 and rpd3 act on ribosomal DNA to control the replication program in budding yeast. Mol Cell. 2014;54(4):691-7. Epub 2014/05/27. doi: 10.1016/j.molcel.2014.04.032. PubMed PMID: 24856221.

6. Ide S, Miyazaki T, Maki H, Kobayashi T. Abundance of ribosomal RNA gene copies maintains genome integrity. Science. 2010;327(5966):693-6. Epub 2010/02/06. doi: 10.1126/science.1179044. PubMed PMID: 20133573.

663 7. Kobayashi T. The replication fork barrier site forms a unique structure with Fob1p and
664 inhibits the replication fork. Mol Cell Biol. 2003;23(24):9178-88. Epub 2003/12/04. PubMed
665 PMID: 14645529; PubMed Central PMCID: PMCPMC309713.
666 8. Kobayashi T, Ganley AR. Recombination regulation by transcription-induced cohesin
667 dissociation in rDNA repeats. Science. 2005;309(5740):1581-4. Epub 2005/09/06. doi:
668 10.1126/science.1116102. PubMed PMID: 16141077.
669 9. Fritze CE, Verschueren K, Strich R, Easton Esposito R. Direct evidence for SIR2
670 modulation of chromatin structure in yeast rDNA. Embo j. 1997;16(21):6495-509. Epub
671 1997/11/14. doi: 10.1093/emboj/16.21.6495. PubMed PMID: 9351831; PubMed Central PMCID:
672 PMCPMC1170255.
673 10. Sandmeier JJ, French S, Osheim Y, Cheung WL, Gallo CM, Beyer AL, et al. RPD3 is
674 required for the inactivation of yeast ribosomal DNA genes in stationary phase. Embo j.
675 2002;21(18):4959-68. Epub 2002/09/18. PubMed PMID: 12234935; PubMed Central PMCID:
676 PMCPMC126294.
677 11. Santoro R, Li J, Grummt I. The nucleolar remodeling complex NoRC mediates
678 heterochromatin formation and silencing of ribosomal gene transcription. Nat Genet.
679 2002;32(3):393-6. Epub 2002/10/09. doi: 10.1038/ng1010. PubMed PMID: 12368916.
680 12. Li J, Langst G, Grummt I. NoRC-dependent nucleosome positioning silences rRNA
681 genes. Embo j. 2006;25(24):5735-41. Epub 2006/12/02. doi: 10.1038/sj.emboj.7601454.
682 PubMed PMID: 17139253; PubMed Central PMCID: PMCPMC1698900.
683 13. Zhang Y, Anderson SJ, French SL, Sikes ML, Viktorovskaya OV, Huband J, et al. The
684 SWI/SNF chromatin remodeling complex influences transcription by RNA polymerase I in
685 Saccharomyces cerevisiae. PLoS One. 2013;8(2):e56793. Epub 2013/02/26. doi:
686 10.1371/journal.pone.0056793. PubMed PMID: 23437238; PubMed Central PMCID:
687 PMCPMC3577654.

14. Jones HS, Kawauchi J, Braglia P, Alen CM, Kent NA, Proudfoot NJ. RNA polymerase I in yeast transcribes dynamic nucleosomal rDNA. Nat Struct Mol Biol. 2007;14(2):123-30. Epub 2007/01/30. doi: 10.1038/nsmb1199. PubMed PMID: 17259992.

15. Fazzio TG, Tsukiyama T. Chromatin remodeling in vivo: evidence for a nucleosome sliding mechanism. Mol Cell. 2003;12(5):1333-40. Epub 2003/11/26. PubMed PMID: 14636590.

16. Goldmark JP, Fazzio TG, Estep PW, Church GM, Tsukiyama T. The Isw2 chromatin remodeling complex represses early meiotic genes upon recruitment by Ume6p. Cell. 2000;103(3):423-33. Epub 2000/11/18. PubMed PMID: 11081629.

17. Fazzio TG, Kooperberg C, Goldmark JP, Neal C, Basom R, Delrow J, et al. Widespread collaboration of Isw2 and Sin3-Rpd3 chromatin remodeling complexes in transcriptional repression. Mol Cell Biol. 2001;21(19):6450-60. Epub 2001/09/05. PubMed PMID: 11533234; PubMed Central PMCID: PMCPMC99792.

18. Whitehouse I, Rando OJ, Delrow J, Tsukiyama T. Chromatin remodelling at promoters suppresses antisense transcription. Nature. 2007;450(7172):1031-5. Epub 2007/12/14. doi: 10.1038/nature06391. PubMed PMID: 18075583.

19. Tsukuda T, Fleming AB, Nickoloff JA, Osley MA. Chromatin remodelling at a DNA double-strand break site in Saccharomyces cerevisiae. Nature. 2005;438(7066):379-83. Epub 2005/11/18. doi: 10.1038/nature04148. PubMed PMID: 16292314; PubMed Central PMCID: PMCPMC1388271.

20. Udugama M, Sabri A, Bartholomew B. The INO80 ATP-dependent chromatin remodeling complex is a nucleosome spacing factor. Mol Cell Biol. 2011;31(4):662-73. Epub 2010/12/08. doi: 10.1128/mcb.01035-10. PubMed PMID: 21135121; PubMed Central PMCID: PMCPMC3028646.

21. Papamichos-Chronakis M, Watanabe S, Rando OJ, Peterson CL. Global regulation of H2A.Z localization by the INO80 chromatin-remodeling enzyme is essential for genome

integrity. Cell. 2011;144(2):200-13. Epub 2011/01/19. doi: 10.1016/j.cell.2010.12.021. PubMed PMID: 21241891; PubMed Central PMCID: PMCPMC3035940.

22. Zhou CY, Johnson SL, Lee LJ, Longhurst AD, Beckwith SL, Johnson MJ, et al. The Yeast INO80 Complex Operates as a Tunable DNA Length-Sensitive Switch to Regulate Nucleosome Sliding. Mol Cell. 2018;69(4):677-88.e9. Epub 2018/02/18. doi: 10.1016/j.molcel.2018.01.028. PubMed PMID: 29452642.

23. Morrison AJ, Highland J, Krogan NJ, Arbel-Eden A, Greenblatt JF, Haber JE, et al. INO80 and gamma-H2AX interaction links ATP-dependent chromatin remodeling to DNA damage repair. Cell. 2004;119(6):767-75. Epub 2004/12/21. doi: 10.1016/j.cell.2004.11.037. PubMed PMID: 15607974.

24. Morrison AJ, Kim JA, Person MD, Highland J, Xiao J, Wehr TS, et al. Mec1/Tel1 phosphorylation of the INO80 chromatin remodeling complex influences DNA damage checkpoint responses. Cell. 2007;130(3):499-511. Epub 2007/08/19. doi: 10.1016/j.cell.2007.06.010. PubMed PMID: 17693258.

25. Shimada K, Oma Y, Schleker T, Kugou K, Ohta K, Harata M, et al. Ino80 chromatin remodeling complex promotes recovery of stalled replication forks. Curr Biol. 2008;18(8):566-75. Epub 2008/04/15. doi: 10.1016/j.cub.2008.03.049. PubMed PMID: 18406137.

26. Vincent JA, Kwong TJ, Tsukiyama T. ATP-dependent chromatin remodeling shapes the DNA replication landscape. Nat Struct Mol Biol. 2008;15(5):477-84. Epub 2008/04/15. doi: 10.1038/nsmb.1419. PubMed PMID: 18408730; PubMed Central PMCID: PMCPMC2678716.

27. Au TJ, Rodriguez J, Vincent JA, Tsukiyama T. ATP-dependent chromatin remodeling factors tune S phase checkpoint activity. Mol Cell Biol. 2011;31(22):4454-63. Epub 2011/09/21. doi: 10.1128/mcb.05931-11. PubMed PMID: 21930788; PubMed Central PMCID: PMCPMC3209248.

28. Smith JS, Boeke JD. An unusual form of transcriptional silencing in yeast ribosomal DNA. Genes Dev. 1997;11(2):241-54. Epub 1997/01/15. PubMed PMID: 9009206.

739 29. Conconi A, Widmer RM, Koller T, Sogo JM. Two different chromatin structures coexist in
740 ribosomal RNA genes throughout the cell cycle. Cell. 1989;57(5):753-61. Epub 1989/06/02.
741 PubMed PMID: 2720786.
742 30. French SL, Osheim YN, Cioci F, Nomura M, Beyer AL. In exponentially growing
743 Saccharomyces cerevisiae cells, rRNA synthesis is determined by the summed RNA
744 polymerase I loading rate rather than by the number of active genes. Mol Cell Biol.
745 2003;23(5):1558-68. Epub 2003/02/18. PubMed PMID: 12588976; PubMed Central PMCID:
746 PMCPMC151703.
747 31. Merz K, Hondele M, Goetze H, Gmelch K, Stoeckl U, Griesenbeck J. Actively
748 transcribed rRNA genes in S. cerevisiae are organized in a specialized chromatin associated
749 with the high-mobility group protein Hmo1 and are largely devoid of histone molecules. Genes
750 Dev. 2008;22(9):1190-204. Epub 2008/05/03. doi: 10.1101/gad.466908. PubMed PMID:
751 18451108; PubMed Central PMCID: PMCPMC2335315.
752 32. Dammann R, Lucchini R, Koller T, Sogo JM. Chromatin structures and transcription of
753 rDNA in yeast Saccharomyces cerevisiae. Nucleic Acids Res. 1993;21(10):2331-8. Epub
754 1993/05/25. PubMed PMID: 8506130; PubMed Central PMCID: PMCPMC309528.
755 33. Woolford JL, Jr., Baserga SJ. Ribosome biogenesis in the yeast Saccharomyces
756 cerevisiae. Genetics. 2013;195(3):643-81. Epub 2013/11/06. doi: 10.1534/genetics.113.153197.
757 PubMed PMID: 24190922; PubMed Central PMCID: PMCPMC3813855.
758 34. Bywater MJ, Poortinga G, Sanij E, Hein N, Peck A, Cullinane C, et al. Inhibition of RNA
759 polymerase I as a therapeutic strategy to promote cancer-specific activation of p53. Cancer
760 Cell. 2012;22(1):51-65. Epub 2012/07/14. doi: 10.1016/j.ccr.2012.05.019. PubMed PMID:
761 22789538; PubMed Central PMCID: PMCPMC3749732.
762 35. Laribee RN, Hosni-Ahmed A, Workman JJ, Chen H. Ccr4-not regulates RNA
763 polymerase I transcription and couples nutrient signaling to the control of ribosomal RNA
764 biogenesis. PLoS Genet. 2015;11(3):e1005113. Epub 2015/03/31. doi:

765 10.1371/journal.pgen.1005113. PubMed PMID: 25815716; PubMed Central PMCID:
766 PMCPMC4376722.
767 36. Beckouet F, Labarre-Mariotte S, Albert B, Imazawa Y, Werner M, Gadal O, et al. Two
768 RNA polymerase I subunits control the binding and release of Rrn3 during transcription. Mol
769 Cell Biol. 2008;28(5):1596-605. Epub 2007/12/19. doi: 10.1128/mcb.01464-07. PubMed PMID:
770 18086878; PubMed Central PMCID: PMCPMC2258765.
771 37. Weiner A, Hughes A, Yassour M, Rando OJ, Friedman N. High-resolution nucleosome
772 mapping reveals transcription-dependent promoter packaging. Genome Res. 2010;20(1):90-
773 100. Epub 2009/10/23. doi: 10.1101/gr.098509.109. PubMed PMID: 19846608; PubMed Central
774 PMCID: PMCPMC2798834.
775 38. Azvolinsky A, Giresi PG, Lieb JD, Zakian VA. Highly transcribed RNA polymerase II
776 genes are impediments to replication fork progression in Saccharomyces cerevisiae. Mol Cell.
777 2009;34(6):722-34. Epub 2009/06/30. doi: 10.1016/j.molcel.2009.05.022. PubMed PMID:
778 19560424; PubMed Central PMCID: PMCPMC2728070.
779 39. Sanij E, Poortinga G, Sharkey K, Hung S, Holloway TP, Quin J, et al. UBF levels
780 determine the number of active ribosomal RNA genes in mammals. J Cell Biol.
781 2008;183(7):1259-74. Epub 2008/12/24. doi: 10.1083/jcb.200805146. PubMed PMID:
782 19103806; PubMed Central PMCID: PMCPMC2606969.
783 40. Jiang C, Pugh BF. Nucleosome positioning and gene regulation: advances through
784 genomics. Nat Rev Genet. 2009;10(3):161-72. Epub 2009/02/11. doi: 10.1038/nrg2522.
785 PubMed PMID: 19204718; PubMed Central PMCID: PMCPMC4860946.
786 41. Rando OJ, Winston F. Chromatin and transcription in yeast. Genetics. 2012;190(2):351-
787 87. Epub 2012/02/22. doi: 10.1534/genetics.111.132266. PubMed PMID: 22345607; PubMed
788 Central PMCID: PMCPMC3276623.

789 42. Simpson RT. Nucleosome positioning can affect the function of a cis-acting DNA
790 element in vivo. Nature. 1990;343(6256):387-9. Epub 1990/01/25. doi: 10.1038/343387a0.
791 PubMed PMID: 2405281.
792 43. Lipford JR, Bell SP. Nucleosomes positioned by ORC facilitate the initiation of DNA
793 replication. Mol Cell. 2001;7(1):21-30. Epub 2001/02/15. PubMed PMID: 11172708.
794 44. Kurat CF, Yeeles JTP, Patel H, Early A, Diffley JFX. Chromatin Controls DNA
795 Replication Origin Selection, Lagging-Strand Synthesis, and Replication Fork Rates. Mol Cell.
796 2017;65(1):117-30. Epub 2016/12/19. doi: 10.1016/j.molcel.2016.11.016. PubMed PMID:
797 27989438; PubMed Central PMCID: PMCPMC5222724.
798 45. Euskirchen GM, Auerbach RK, Davidov E, Gianoulis TA, Zhong G, Rozowsky J, et al.
799 Diverse roles and interactions of the SWI/SNF chromatin remodeling complex revealed using
800 global approaches. PLoS Genet. 2011;7(3):e1002008. Epub 2011/03/17. doi:
801 10.1371/journal.pgen.1002008. PubMed PMID: 21408204; PubMed Central PMCID:
802 PMCPMC3048368.
803 46. Flanagan JF, Peterson CL. A role for the yeast SWI/SNF complex in DNA replication.
804 Nucleic Acids Res. 1999;27(9):2022-8. Epub 1999/04/13. PubMed PMID: 10198436; PubMed
805 Central PMCID: PMCPMC148416.
806 47. Azmi IF, Watanabe S, Maloney MF, Kang S, Belsky JA, MacAlpine DM, et al.
807 Nucleosomes influence multiple steps during replication initiation. Elife. 2017;6. Epub
808 2017/03/23. doi: 10.7554/eLife.22512. PubMed PMID: 28322723; PubMed Central PMCID:
809 PMCPMC5400510.
810 48. Muller M, Lucchini R, Sogo JM. Replication of yeast rDNA initiates downstream of
811 transcriptionally active genes. Mol Cell. 2000;5(5):767-77. Epub 2000/07/06. PubMed PMID:
812 10882113.
813 49. Salim D, Bradford WD, Freeland A, Cady G, Wang J, Pruitt SC, et al. DNA replication
814 stress restricts ribosomal DNA copy number. PLoS Genet. 2017;13(9):e1007006. Epub

2017/09/16. doi: 10.1371/journal.pgen.1007006. PubMed PMID: 28915237; PubMed Central PMCID: PMCPMC5617229.

50. Kobayashi T, Heck DJ, Nomura M, Horiuchi T. Expansion and contraction of ribosomal DNA repeats in Saccharomyces cerevisiae: requirement of replication fork blocking (Fob1) protein and the role of RNA polymerase I. Genes Dev. 1998;12(24):3821-30. Epub 1998/12/31. PubMed PMID: 9869636; PubMed Central PMCID: PMCPMC317266.

51. Brewer BJ, Lockshon D, Fangman WL. The arrest of replication forks in the rDNA of yeast occurs independently of transcription. Cell. 1992;71(2):267-76. Epub 1992/10/16. PubMed PMID: 1423594.

52. Sanchez JC, Kwan EX, Pohl TJ, Amemiya HM, Raghuraman MK, Brewer BJ. Defective replication initiation results in locus specific chromosome breakage and a ribosomal RNA deficiency in yeast. PLoS Genet. 2017;13(10):e1007041. Epub 2017/10/17. doi: 10.1371/journal.pgen.1007041. PubMed PMID: 29036220; PubMed Central PMCID: PMCPMC5658192.

53. Papamichos-Chronakis M, Krebs JE, Peterson CL. Interplay between Ino80 and Swr1 chromatin remodeling enzymes regulates cell cycle checkpoint adaptation in response to DNA damage. Genes Dev. 2006;20(17):2437-49. Epub 2006/09/05. doi: 10.1101/gad.1440206. PubMed PMID: 16951256; PubMed Central PMCID: PMCPMC1560417.

54. Lademann CA, Renkawitz J, Pfander B, Jentsch S. The INO80 Complex Removes H2A.Z to Promote Presynaptic Filament Formation during Homologous Recombination. Cell Rep. 2017;19(7):1294-303. Epub 2017/05/18. doi: 10.1016/j.celrep.2017.04.051. PubMed PMID: 28514650.

55. Ganley AR, Ide S, Saka K, Kobayashi T. The effect of replication initiation on gene amplification in the rDNA and its relationship to aging. Mol Cell. 2009;35(5):683-93. Epub 2009/09/15. doi: 10.1016/j.molcel.2009.07.012. PubMed PMID: 19748361.

840 56. Thomas BJ, Rothstein R. The genetic control of direct-repeat recombination in
841 Saccharomyces: the effect of rad52 and rad1 on mitotic recombination at GAL10, a
842 transcriptionally regulated gene. Genetics. 1989;123(4):725-38. Epub 1989/12/01. PubMed
843 PMID: 2693208; PubMed Central PMCID: PMCPMC1203884.
844 57. Zhao X, Muller EG, Rothstein R. A suppressor of two essential checkpoint genes
845 identifies a novel protein that negatively affects dNTP pools. Mol Cell. 1998;2(3):329-40. Epub
846 1998/10/17. PubMed PMID: 9774971.
847 58. Rodriguez J, McKnight JN, Tsukiyama T. Genome-Wide Analysis of Nucleosome
848 Positions, Occupancy, and Accessibility in Yeast: Nucleosome Mapping, High-Resolution
849 Histone ChIP, and NCAM. Curr Protoc Mol Biol. 2014;108:21.8.1-16. Epub 2014/10/02. doi:
850 10.1002/0471142727.mb2128s108. PubMed PMID: 25271716; PubMed Central PMCID:
851 PMCPMC4183977.
852 59. Gelbart ME, Bachman N, Delrow J, Boeke JD, Tsukiyama T. Genome-wide identification
853 of Isw2 chromatin-remodeling targets by localization of a catalytically inactive mutant. Genes
854 Dev. 2005;19(8):942-54. Epub 2005/04/19. doi: 10.1101/gad.1298905. PubMed PMID:
855 15833917; PubMed Central PMCID: PMCPMC1080133.
856 60. Kwan EX, Wang XS, Amemiya HM, Brewer BJ, Raghuraman MK. rDNA Copy Number
857 Variants Are Frequent Passenger Mutations in Saccharomyces cerevisiae Deletion Collections
858 and de Novo Transformants. G3 (Bethesda). 2016;6(9):2829-38. Epub 2016/07/28. doi:
859 10.1534/g3.116.030296. PubMed PMID: 27449518; PubMed Central PMCID:
860 PMCPMC5015940.
861
862
863
864

Supporting Information

S1 Fig. Striking nucleosome positioning changes at a canonical Isw2 target. (A) MNase-seq data at a well-established Isw2 target, the 5' end of the *POT1* gene. (B) Visualization of the same data shown in S2A Fig with the ribbon plots used in Fig 3B, focusing on two pairs of nucleosomes.

S2 Fig. Nucleosome positioning in single and double mutants throughout the rDNA. (A) MNase-seq data analyzed with dyad mapping showing the entire 35S rRNA gene. No clear differences in nucleosome positioning can be seen. (B) Ribbon plot of the same MNase-seq data focused on the 5S-adjacent nucleosome. In wild-type cells and *isw2*Δ and *nhp10*Δ cells, sub-species *a* is higher than sub-species *b*, while in *isw2*Δ *nhp10*Δ cells the *b* peak is higher than for *a*. (C) RNA Pol III ChIP-seq at the Pol III-transcribed 5S gene showing no appreciable difference in levels of the polymerase between wild-type and *isw2*Δ *nhp10*Δ cells. (D) MNase-seq ribbon plot at the 35S promoter region showing no appreciable difference in nucleosome positioning across the strains tested.

S3 Fig. Different MNase digestions. (D) Representative gel indicating how nucleosomal ladders appear after digestion with 20, 40, or 80 units of MNase. Note that for all MNase-seq analyses, regardless of level of digestion, the mono-nucleosomal band was gel-purified and was the sole source of material subjected to deep sequencing.

S4 Fig. DNA polymerase pausing does not vary between tested strains at a known pause site, *PDC1*. ChIP-seq of DNA polymerase epsilon subunit Pol2 at the *PDC1* gene, a site known

to show polymerase pausing by this method (Azvolinsky 2009). Levels of Pol2 do not appreciably vary across the strains tested.

S5 Fig. Isw2 and Ino80 affect depth of the 35S promoter's nucleosome depleted region. The same H3 ChIP-seq data shown in Fig 2A, zoomed in on the 35S promoter region (Y axis on log2 scale). Depth of the NDR is appreciably greater in *isw2*Δ *nhp10*Δ cells than in wild-type cells, and NDR depth is at an intermediate level in single mutant cells.

S1 Table. List of yeast strains used.

S2 Table. List of PCR primers used.

S3 Table. List of plasmids used.

Figure Captions

Fig 1. The Isw2 and Ino80 chromatin remodeling complexes are targeted to the rDNA locus. (A) A schematic drawing of the rDNA locus in *S. cerevisiae*. In a typical yeast cell, the rDNA accounts for approximately 1.5 Mb of chromosome XII, comprised of a tandem array of ~150 copies of the rDNA repeat. Each repeat contains a 35S rRNA gene and an inter-genic spacer (IGS) region in between adjacent 35S genes, itself split into IGS1 and IGS2 regions by the 5S rRNA gene. IGS1 contains the ribosomal origin of replication, or autonomously replicating sequence (rARS), and IGS2 contains the bi-directional RNA Polymerase II promoter, E-pro, and a replication fork block (RFB). (B) The Isw2 subunit of the Isw2 complex and the

914 Nhp10 subunit of the Ino80 complex were each FLAG-tagged, chromatin immuno-precipitated,
915 and deep-sequenced (ChIP-seq). (C) Representative ChIP-seq signals of Isw2 and Nhp10 at
916 single copy targets outside of the rDNA.
917
918
919 **Fig 2. Nucleosome occupancy, but not transcription, is affected at the 35S rDNA in *isw2*Δ**
920 **and *nhp10*Δ mutants.**
921 (A) Histone H3 ChIP-seq through the 35S rRNA gene. Line represents average log2 ChIP-seq
922 signal at each base pair for two independent experiments, and the ribbon represents the
923 standard error of the mean at each base pair. Schematic drawing of the 35S includes
924 transcribed spacers that are removed during processing, as well as the mature 18S, 5.8S, and
925 25S rRNAs that are parts of complete ribosomes. ETS1 and ITS1 qPCR primer sets are
926 indicated with red lines, and ETS1 hybridization probe, used in the Southern blot shown in 2B,
927 indicated in green. In this and all following figures, “wild-type” has been abbreviated as “WT”.
928 (B) Psoralen cross-linked DNA, digested with EcoRI and hybridized with a probe to the ETS1
929 region. Psoralen incorporates more readily into nucleosome-occupied, actively transcribed
930 rDNA repeats, causing these bands to migrate more slowly than nucleosome-depleted, inactive
931 repeats. Two independent isolates of each remodeling factor mutant are shown. For
932 quantification, mean intensity of each band was measured with ImageJ software. Values for
933 each genotype reflect between 3 and 5 biological replicates, and error bars represent standard
934 error of the mean. (C) RT-qPCR measuring the ETS1 and ITS1 of the 35S pre-rRNA. (D) RNA
935 Pol I ChIP-seq.
936
937 **Fig 3. Isw2 and Ino80 affect nucleosome positioning in the rDNA inter-genic spacer.**
938 (A) Micrococcal nuclease digestion followed by deep-sequencing (MNase-seq) profiles in the
939 IGS, with Isw2 ChIP-seq data overlaid. From each paired end sequencing read, the nucleosome

dyad was inferred and plotted. (B) Ribbon plots, generated as described in Fig 2A, focused on two pairs of nucleosomes, indicated with boxes in Fig 3A. Each of the four tested strains has a characteristic profile of positioning at each of these four nucleosomes. Different sub-species of nucleosome positions are indicated with colored arrows and letters. (C) MNase-seq comparing wild-type and *isw2*Δ *nhp10*Δ cells across three different strengths of MNase digestion. (D) Cartoon depicting different nucleosomal sub-species, highlighting the most striking differences in sub-species profiles between wild-type and *isw2*Δ *nhp10*Δ cells.

Fig 4. Isw2 and Ino80 facilitate efficient firing of rDNA origin of replication.

(A) Schematic drawing of 2D gel with features annotated. The 1N spot is comprised of restriction fragments that are not in the process of replicating; the Y arc of restriction fragments that are being passively replicated; and the bubble arc of restriction fragments in which an origin of replication has actively fired. Replication fork pausing at the RFB causes an accumulation of restriction fragments with a specific size and shape, visible as a dark spot on the left arm of the Y-arc. The ratio of bubble arc to Y arc signal is indicative of the ratio of actively to passively replicated restriction fragments, and thus of origin efficiency. (B) Representative 2D gels over rDNA ARS and RFB. Exposures of the blots have been adjusted so that the Y arc is of comparable intensity for each blot, such that direct comparison of bubble arc intensity across images is equivalent to a comparison of bubble-to-Y ratio. Bubble arc indicated by empty arrow, Y arc indicated by filled arrow. Quantification based on measurement of average intensity of arcs using ImageQuantTL software, and reflects at least two independent experiments for each genotype. All values normalized to the bubble:Y ratio for wild-type. Error bars show standard error of the mean. (C) Representative lightly exposed 2D gel images to allow visualization of the 1N and RFB spots.

Fig 5. Isw2 and Ino80 affect replication fork pausing and Fob1 occupancy at the RFB.

(A) ChIP-seq of DNA Polymerase Epsilon subunit Pol2 at the RFB. Ribbon plot produced as described in Fig 2A based on two biological replicates per genotype. Quantification produced by integrating the ChIP-seq signal for each strain across the RFB, and then averaging the results across two replicates. Error bars represent the standard error of the mean. (B) ChIP-qPCR of Fob1 with primers flanking the RFB and within ETS1, all normalized to occupancy at the RFB in wild-type cells. Fob1 is not expected to bind to ETS1, and thus it serves as a negative control locus. Error bars represent standard error of the mean for at least three replicates per genotype.

Fig 6. Isw2 and Ino80 affect the rate of rDNA copy number change.

(A) rDNA copy number change assay. Blue bars indicate *fob1* copy number control strains that stably contain the indicated number of rDNA repeats (identical 150-copy control samples run on both ends of the gel to facilitate comparison of band migration). The gray bar denotes samples grown in a time course for the indicated number of generations, in selective medium to ensure retention of either a plasmid containing *FOB1* (green bar) or the plasmid backbone pRS426 without *FOB1* (red bar). (B) Quantification of the copy number change assay. Average copy numbers at each time point were calculated based on migration of bands relative to controls.

Fig 1

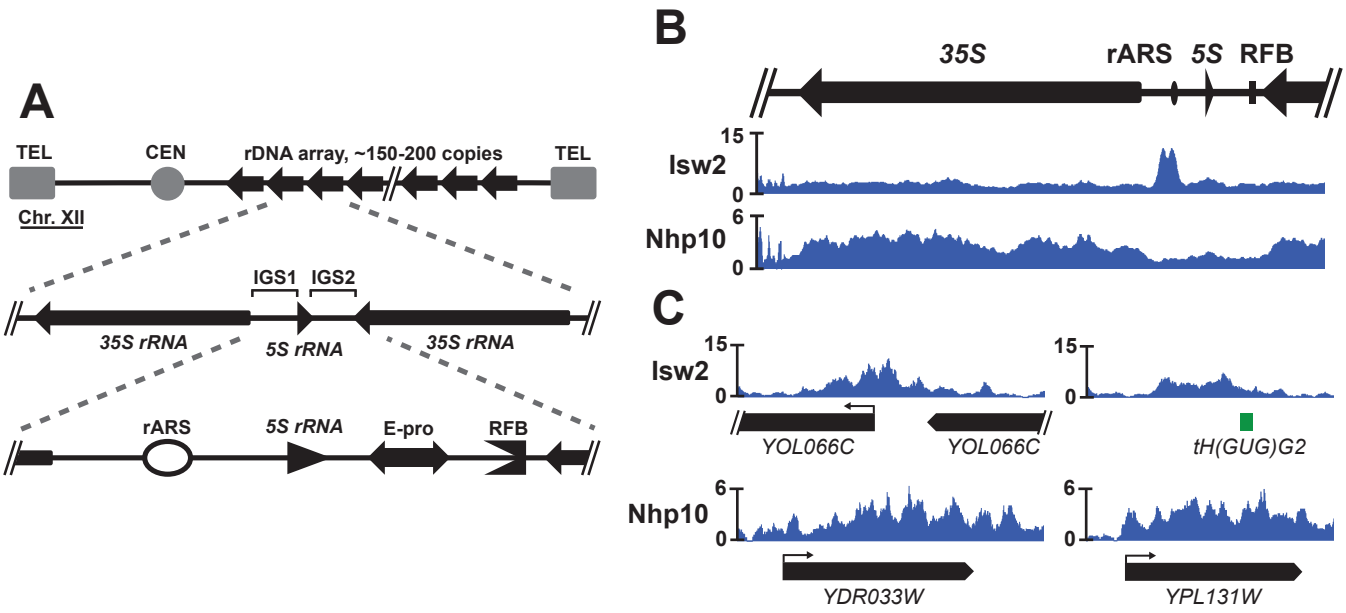

Fig 2

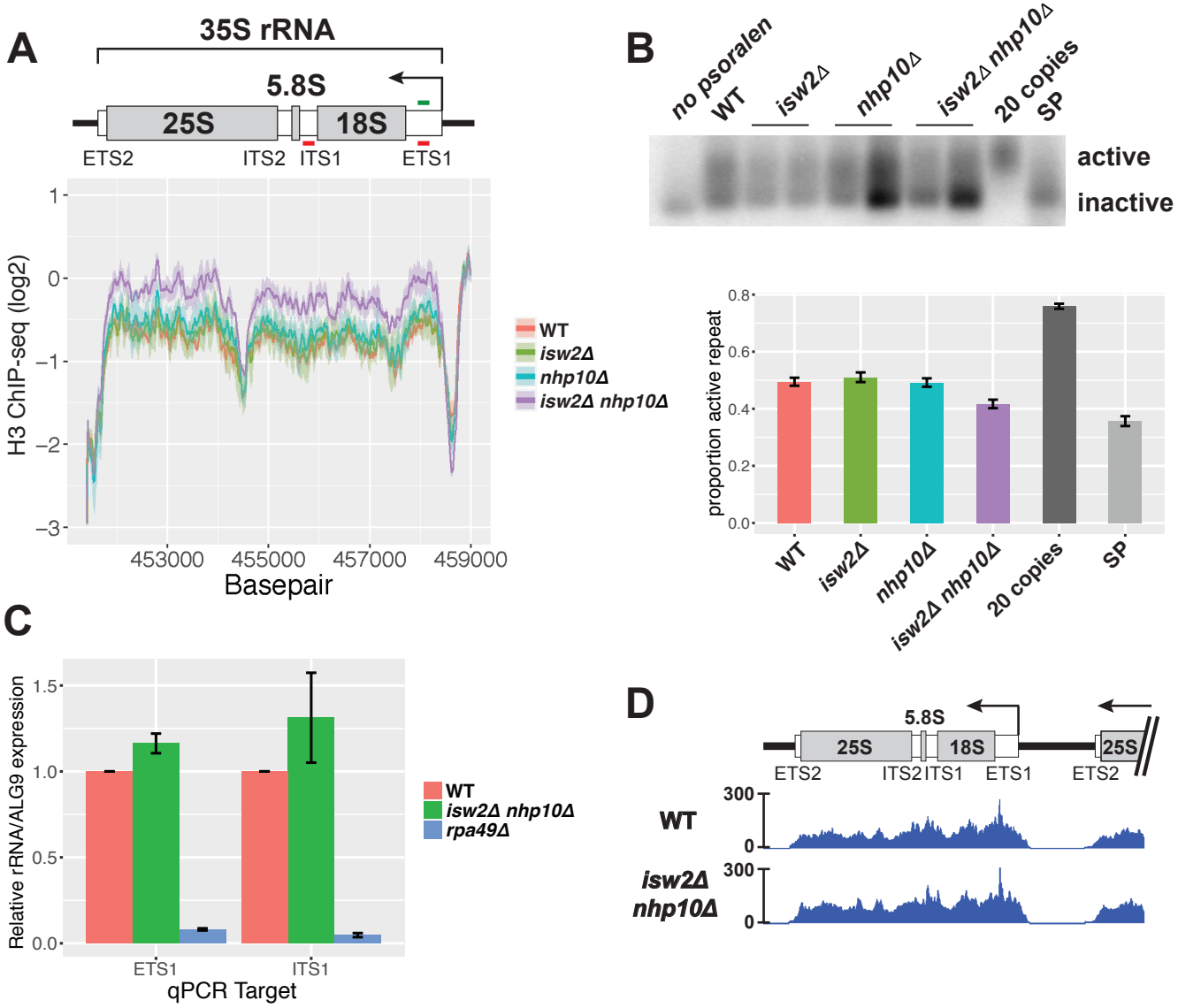

Fig 3

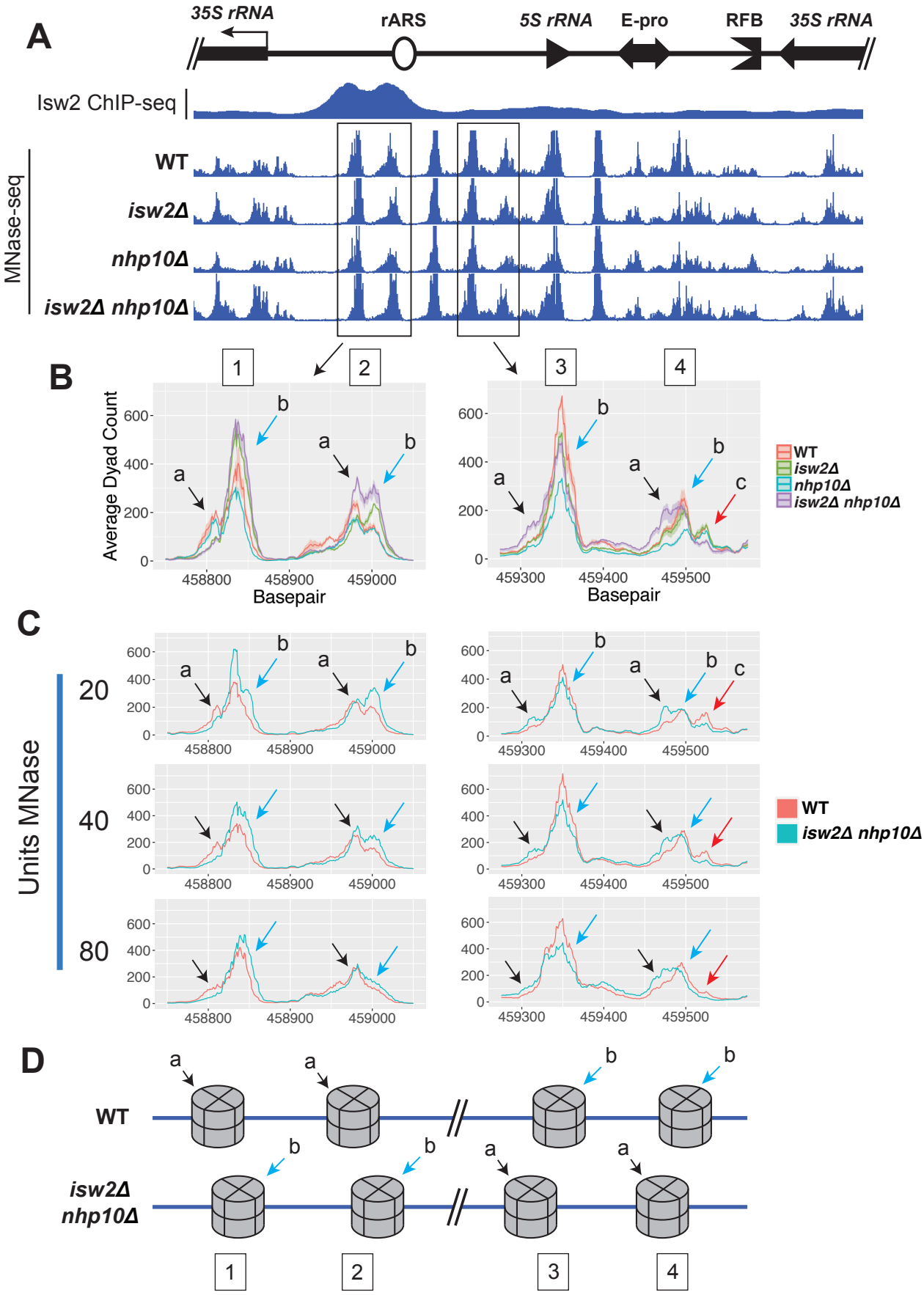

Fig 4

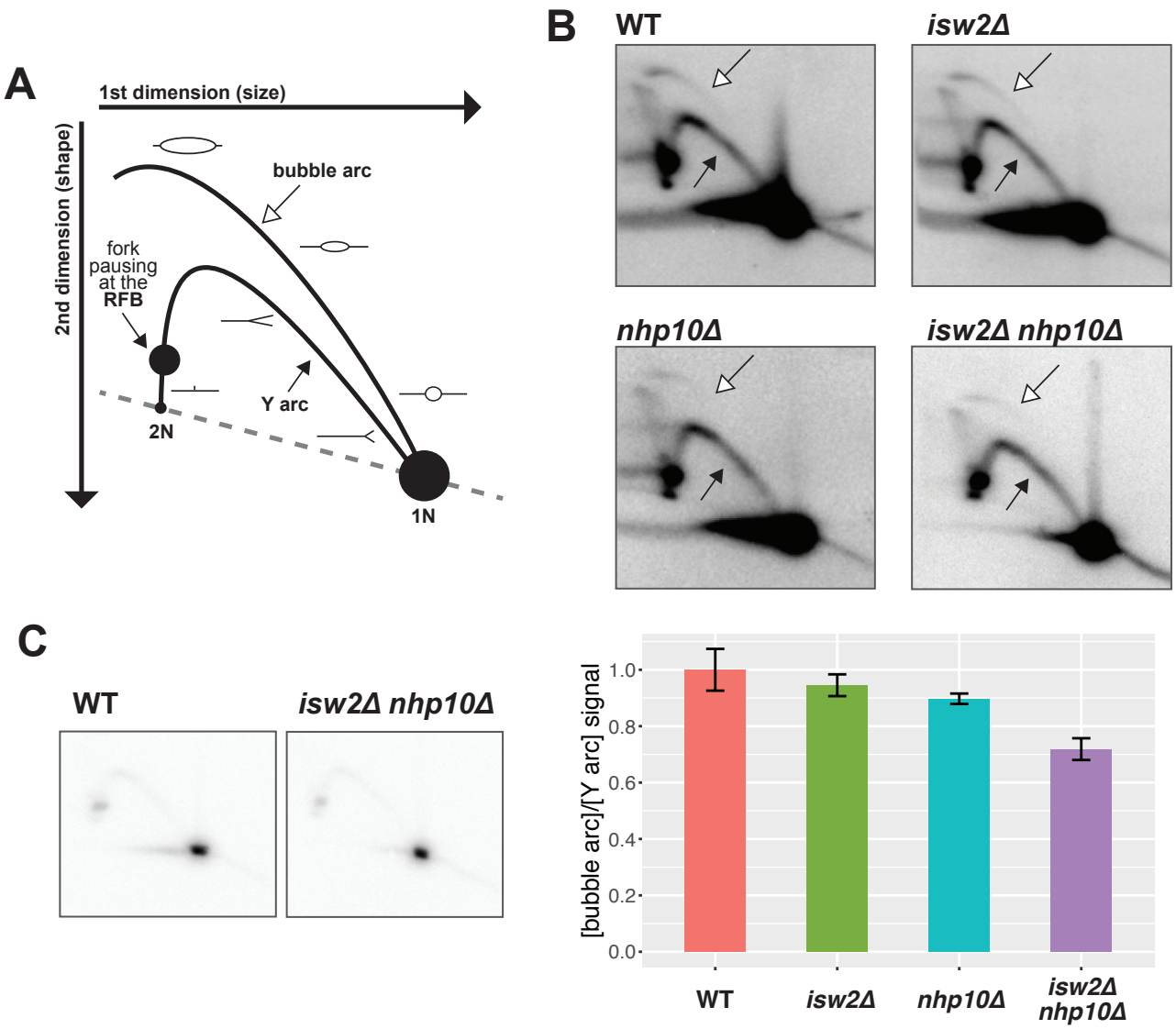

Fig 5

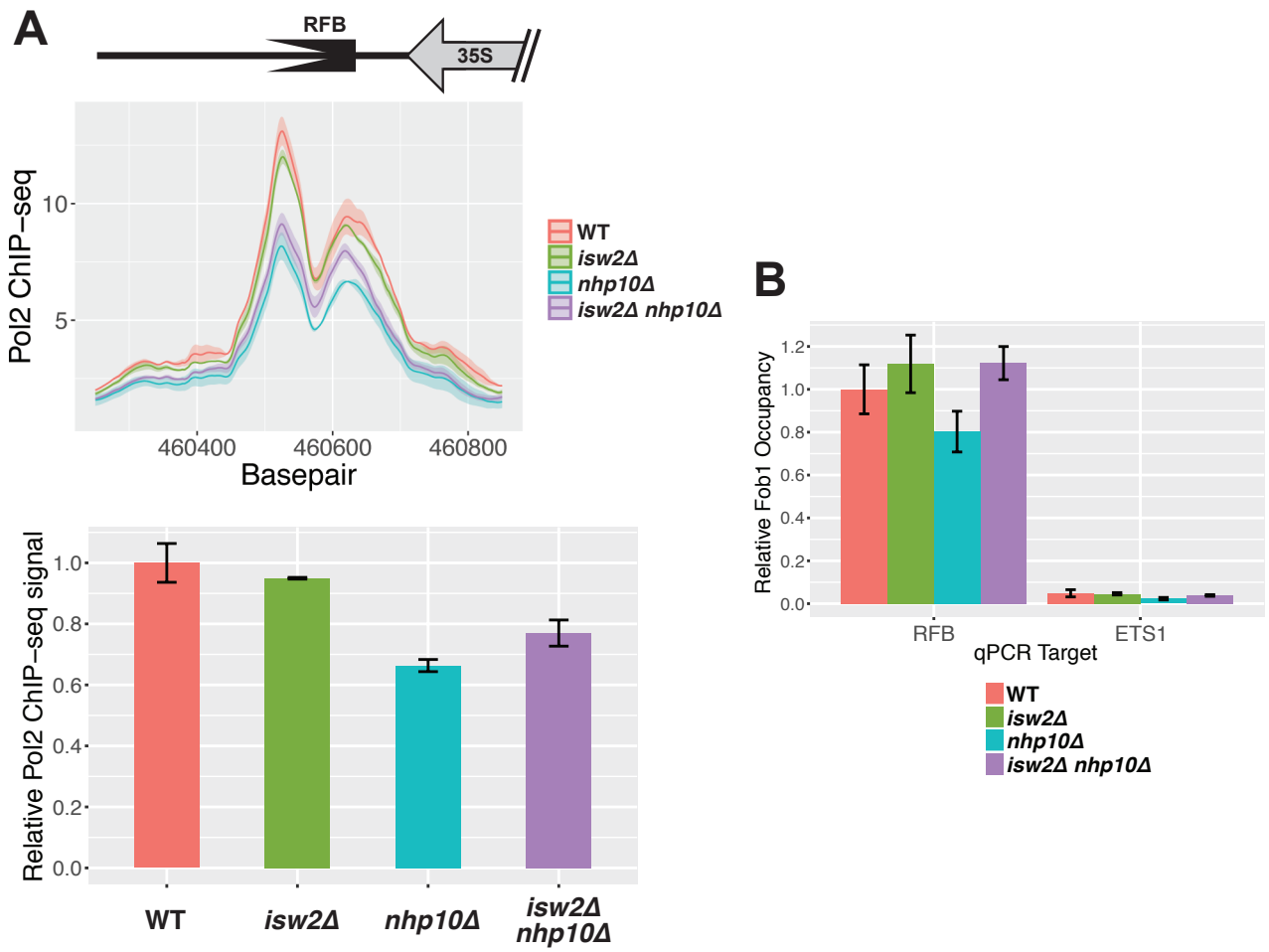

Fig 6

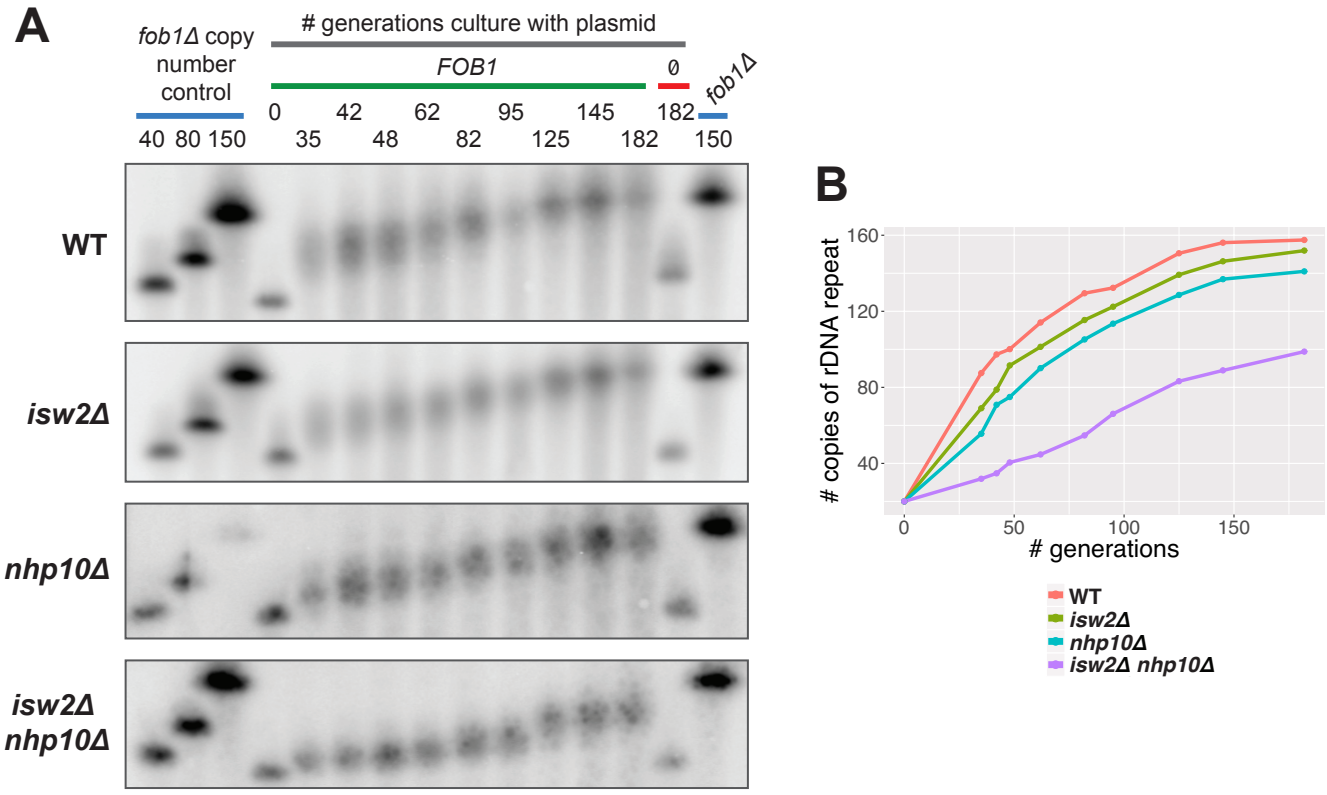

Supplemental 1

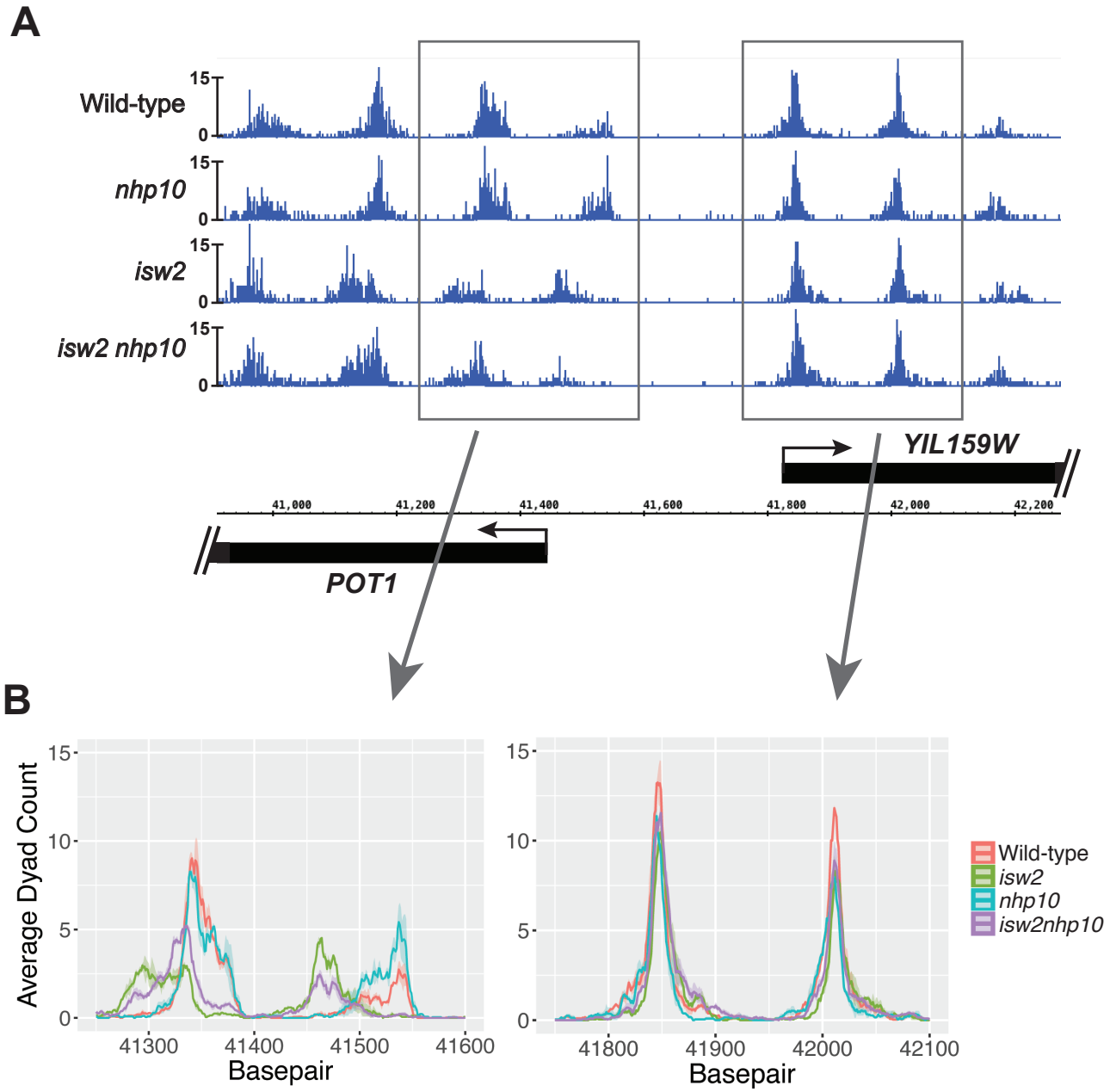

Supplemental 2

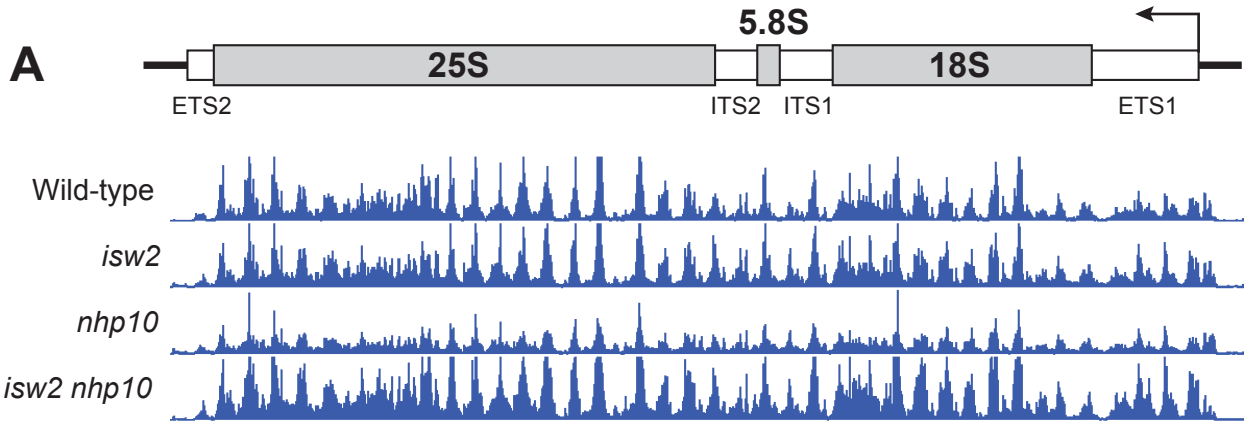

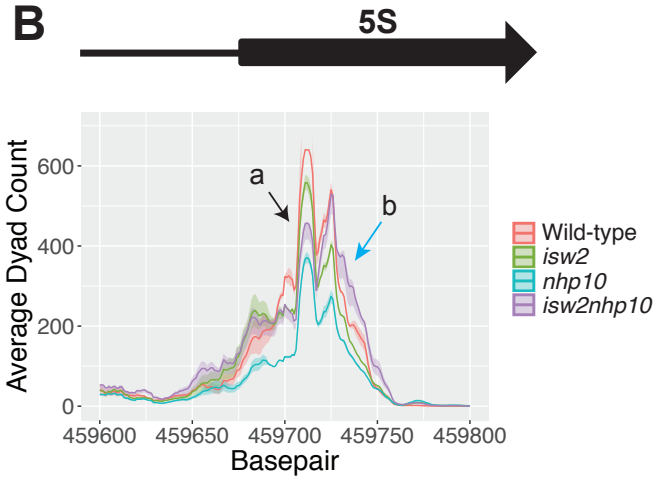

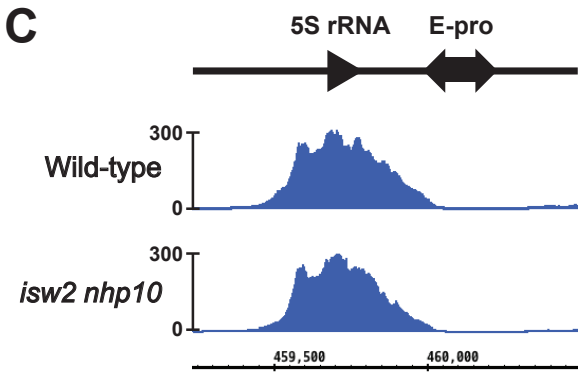

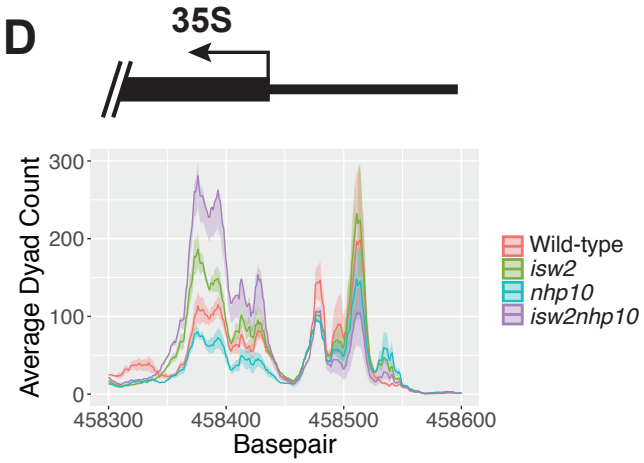

Supplemental 3

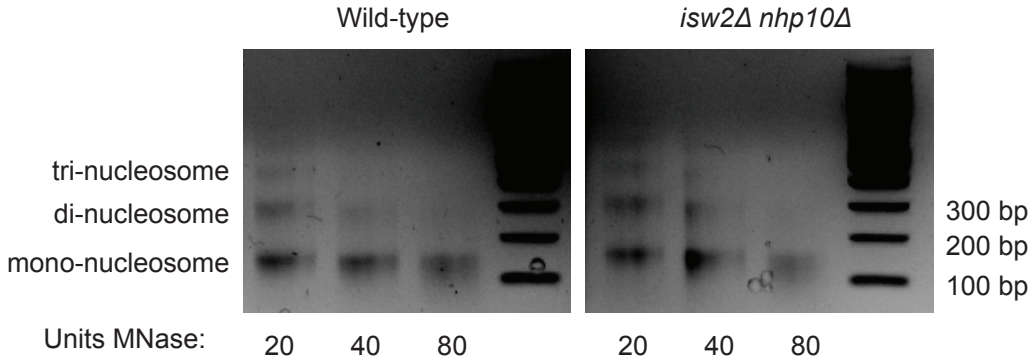

Supplemental 4

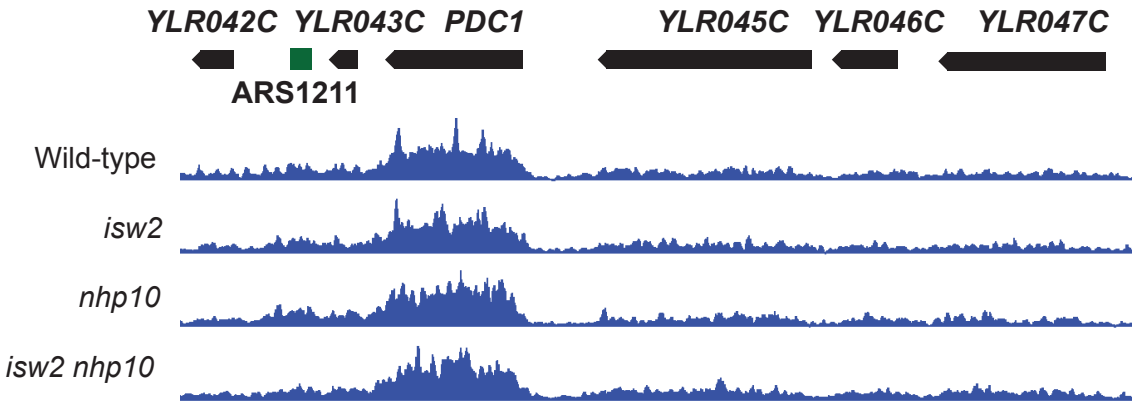

Supplemental 5

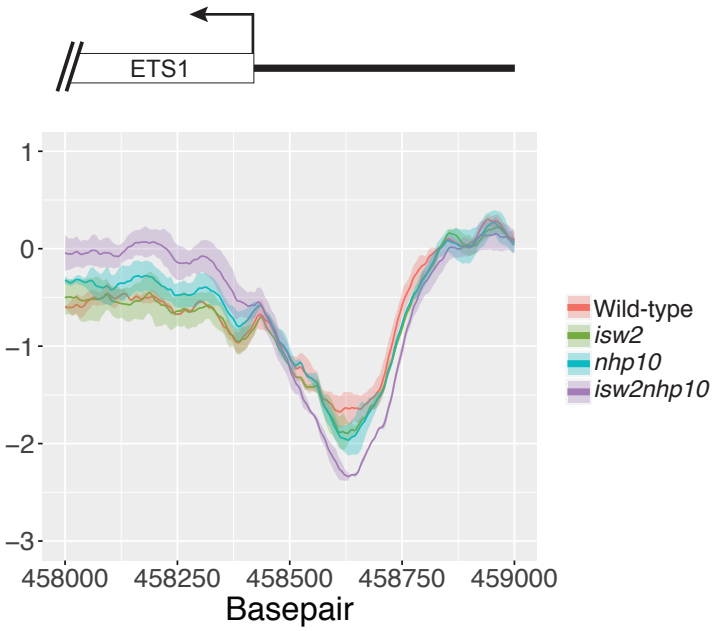

S1 Table. Yeast strains used in this study.

Strain	Genotype	Reference
W1588-4C	*MAT***a** *ade2-1 can1-100 his3-11,15 leu2-3,112 trp1-1 ura3-1*	Thomas and Rothstein 1989, Zhao *et al* 1998
YTT3320	W1588-4C; *isw2Δ::NatMX*	Au *et al* 2011
YTT6809	W1588-4C; *isw2Δ::NatMX*	this study
YTT3333	W1588-4C; *nhp10Δ::Hyg*	Au *et al* 2011
YTT2060	W1588-4C; *nhp10Δ::Hyg*	Vincent *et al* 2008
YTT3337	W1588-4C; isw2Δ::NatMX nhp10Δ::HYG	Au *et al* 2011
YTT2109	W1588-4C; *isw2Δ::NatMX nhp10Δ::HYG*	Vincent *et al* 2008
YTT1996	W1588-4C; *ISW2-K215R-3FLAG-KanMX*	Gelbart *et al* 2005
YTT1997	W1588-4C; *ISW2-K215R-3FLAG-KanMX*	Gelbart *et al* 2005
YTT3426	W1588-4C; *NHP10-3FLAG-KanMX*	Vincent *et al* 2008
YTT3427	W1588-4C; *NHP10-3FLAG-KanMX*	Vincent *et al* 2008
YTT6639	W1588-4C; *rpa49Δ::KanMX*	this study
YTT6673	W1588-4C; *isw2Δ::NatMX nhp10Δ::Hyg RPA190-2L-3FLAG::KanMX*	this study
YTT6679	W1588-4C; *RPA190-2L-3FLAG::KanMX*	this study
YTT6686	W1588-4C; *RPO31-2L-3FLAG::KanMX*	this study
YTT6693	W1588-4C; *isw2Δ::NatMX nhp10Δ::Hyg RPO31-2L-3FLAG::KanMX*	this study
YTT6915	W1588-4C; *Pol2-2L-3FLAG::KanMX*	this study
YTT6916	W1588-4C; *Pol2-2L-3FLAG::KanMX*	this study
YTT6917	W1588-4C; *isw2Δ::NatMX Pol2-2L-3FLAG::KanMX*	this study
YTT6918	W1588-4C; *isw2Δ::NatMX Pol2-2L-3FLAG::KanMX*	this study
YTT6919	W1588-4C; *nhp10Δ::Hyg Pol2-2L-3FLAG::KanMX*	this study
YTT6920	W1588-4C; *nhp10Δ::Hyg Pol2-2L-3FLAG::KanMX*	this study
YTT6921	W1588-4C; *isw2Δ::NatMX nhp10Δ::Hyg Pol2-2L-3FLAG::KanMX*	this study
YTT6922	W1588-4C; *isw2Δ::NatMX nhp10Δ::Hyg Pol2-2L-3FLAG::KanMX*	this study
YTT7009	W1588-4C; *Fob1-2L-3FLAG::KanMX*	this study
YTT7010	W1588-4C; *Fob1-2L-3FLAG::KanMX*	this study
YTT7011	W1588-4C; *isw2Δ::NatMX Fob1-2L-3FLAG::KanMX*	this study
YTT7012	W1588-4C; *isw2Δ::NatMX Fob1-2L-3FLAG::KanMX*	this study
YTT7013	W1588-4C; *nhp10Δ::Hyg Fob1-2L-3FLAG::KanMX*	this study
YTT7014	W1588-4C; *nhp10Δ::Hyg Fob1-2L-3FLAG::KanMX*	this study
YTT7015	W1588-4C; *isw2Δ::NatMX nhp10Δ::Hyg Fob1-2L-3FLAG::KanMX*	this study
YTT7016	W1588-4C; *isw2Δ::NatMX nhp10Δ::Hyg Fob1-2L-3FLAG::KanMX*	this study
YSI101	*MAT***a** *ade2-1 can1-100 his3-11,15 leu2-3,112 trp1-1 ura3-1 fob1::LEU2*	Ide *et al* 2010
YSI102	YSI101; 20 copies rDNA	Ide *et al* 2010
YSI103	YSI101; 40 copies rDNA	Ide *et al* 2010
YSI104	YSI101; 80 copies rDNA	Ide *et al* 2010
YTT6294	YSI102; isw2Δ::NatMX	this study
YTT6865	YSI102; nhp10Δ::HYG	this study
YTT6311	YSI102; isw2Δ::NatMX nhp10Δ::Hyg	this study
YTT6312	YSI102; isw2Δ::NatMX nhp10Δ::Hyg	this study

S2 Table. Primers used in this study.

Name	Comment	Sequence
ETS1-1	5' ETS1 qPCR	TGGGTTGATGCGTATTGAGA
ETS1-2	3' ETS1 qPCR	TCGCTGATTTGAGAGGAGGT
ALG9-1	5' ALG9 qPCR	CACGGATAGTGGCTTTGGTGAACAATTAC [1]
ALG9-2	3' ALG9 qPCR	TATGATTATCTGGCAGCAGGAAAGAACTTGGG [1]
ITS1-6	5' ITS1 qPCR	TGTTTTGGCAAGAGCATGAG
ITS1-7	3' ITS1 qPCR	TCGAATGCCCAAAGAAAAAG
RFB-1	5' RFB qPCR, probe	gcggggtctagaCCACTGTTCACTGTTCACTGTTCA
RFB-2	3' RFB qPCR, probe	cccggcgctagcAGAGAAGGGCTTTCACAAAGCT
rDNA_ETS1-1	5' ETS1 probe	CCATTCCGTGAAACACC
rDNA_ETS1-2	3' ETS1 probe	AAGAAAGAAACCGAAATCTC
AG_Fob1_1	5' Fob1 Gibson cloning (insert)	ctcactatagggcgaattgggtaccgggccTTAATAATGTACTTTGCAGATGTTTGTTCC
AG_Fob1_3	3' Fob1 Gibson cloning (insert)	cgcggtggcggccgctctagaactagtggaCTAATGATAATGGCTTTCTATTTGTTTTGC
AG_Fob1_2	5' Fob1 Gibson cloning (vector)	GGAACAAACATCTGCAAAGTACATTATTAAggcccggtacccaattcgccctatagtgag
AG_Fob1_4	3' Fob1 Gibson cloning (vector)	GCAAAACAAATAGAAAGCCATTATCATTAGtccactagttctagagcggccgccaccgcg

1. Teste MA, Duquenne M, Francois JM, Parrou JL. Validation of reference genes for quantitative expression analysis by real-time RT-PCR in Saccharomyces cerevisiae. BMC Mol Biol. 2009;10:99. Epub 2009/10/31. doi: 10.1186/1471-2199-10-99. PubMed PMID: 19874630; PubMed Central PMCID: PMCPMC2776018.

S3 Table. Plasmids used in this study.

Name	Description
pRS426	URA3, 2μ
pRS426-Fob1	pRS426 with *FOB1* promoter and coding region